Lightweight and Faithful Visual Condition Checking in Behavior Trees via Expert-Regularized Reinforcement Learning

Hyosik Moon, Eldan Cohen

Department of Mechanical and Industrial Engineering
University of Toronto, Toronto, Canada
hyosik.moon@mail.utoronto.ca, eldan.cohen@utoronto.ca

Abstract

Behavior trees provide a transparent and modular structure for encoding expert-designed policies, enabling interpretable decision-making in complex tasks. Yet, applying behavior trees to high-dimensional perceptual inputs such as images or language is challenging as defining symbolic predicates over raw perceptual data is non-trivial. While state-of-the-art large multimodal models (such as vision-language models) can overcome this issue by utilizing natural language queries over perceptual inputs, they incur high computational cost, making them unsuitable for many applications. Imitation learning offers a way to distill these experts into compact models, though it requires extensive supervision. In contrast, reinforcement learning reduces the need for costly supervision but risks misalignment of condition nodes with their intended semantics as well as poor credit assignment. To address these challenges, we introduce **CERL** (Condition-node Expert-regularized Reinforcement Learning), a framework that leverages expert-regularized reinforcement learning to preserve semantic faithfulness, while employing a factorized policy that aggregates sequential condition-node decisions into a single decision unit to alleviate credit assignment challenges. Experiments across seven tasks from the GymCards, FrozenLake, and BabyAIText suites demonstrate that our framework outperforms pure imitation learning or reinforcement learning baselines, retains strong agreement with expert decisions, and achieves substantial gains in inference speed and model size over expert models.

Introduction

Behavior Trees (BTs) (Colledanchise and Ögren 2018; Iovino et al. 2022) are widely valued for their transparency, modularity, and reusability, and they are commonly used to encode expert-designed policies in robotics (Ögren and Sprague 2022; Ghzouli et al. 2020), game AI (Marcotte and Hamilton 2017), and autonomous systems (Hu et al. 2021). Despite these strengths, their applicability to environments with rich perceptual inputs, such as images or natural language, remains limited. Standard BTs are inherently designed to operate on explicit, semantically meaningful features, yet extracting such features from high-dimensional sensory data at each step of a decision sequence is non-trivial. As a result, most BT applications rely on hand-crafted symbolic conditions or carefully engineered features, and only a few recent studies have attempted to extend BTs to perceptual inputs, either through feature engineering (Colledanchise, Parasuraman, and Ögren 2018) or by leveraging large vision–language models (VLMs) for condition evaluation (Wake et al. 2025).

In particular, VLMs (Ghosh et al. 2024) enable the evaluation of natural language condition queries directly on raw perceptual inputs, avoiding manual feature engineering. However, relying on a VLM for every decision during sequential decision-making is often impractical due to computationally expensive inference and the high cost of expert queries (e.g., API calls). A potential workaround is to utilize imitation learning (IL) (Zare et al. 2024) to train a compact condition-node policies based on VLM-labeled condition evaluation data, which can significantly reduce inference costs. Nonetheless, applying IL in the context of BTs poses significant challenge: IL methods typically require large amounts of labeled data, and in BTs this demand is further amplified because each environment action depends on multiple condition-node decisions along the traversal. As a result, IL can still be prohibitively expensive for applications with limited budgets.

An alternative to IL is to use reinforcement learning (RL) to train compact condition-node policies directly from task completion rewards, thereby avoiding expensive VLM-based labeling. However, this approach faces two key challenges. First, optimizing solely based on rewards can cause semantic drift, where condition-node outputs diverge from their intended semantics and instead prioritize reward-maximizing behaviors (Skalse et al. 2022). This undermines the original goal of BTs – transparent and interpretable decision logic through alignment with expert-designed conditions – since the learned nodes may no longer faithfully represent their intended meaning. Second, in sequential structures such as BTs, RL faces credit assignment challenges in sparse-reward settings, because each environment action is determined by a sequence of condition-node decisions, making it especially difficult to assign credit to these individual decision states.

Our framework addresses the first challenge – semantic drift – by incorporating expert regularization during RL, using a limited set of labeled expert decisions to preserve alignment with the intended conditions and prevent the

learned policy from prioritizing reward at the cost of breaking BT semantics. The second challenge – credit assignment in BTs – is alleviated via a theoretically-justified factorized policy that aggregates condition-node decisions for an action as a single decision unit, improving learning signal propagation. Building on these principles, we introduce **CERL** (Condition-node Expert-regularized Reinforcement Learning), a framework that trains condition nodes directly from perceptual inputs through expert-regularized reinforcement learning, ensuring semantic faithfulness and robust learning under sparse rewards.

Our contributions are as follows: (1) we present a novel Markov Decision Process formulation and policy gradient derivation for RL-based training of condition nodes in BT; (2) we propose a unified framework that integrates IL and RL via expert regularization. Our method uses a limited set of expert labels (e.g., from a large VLM) both to initialize and continuously regularize the RL-based training of condition nodes, reducing expert labeling costs while preserving faithfulness to expert decisions; (3) we show that our method substantially improves over IL or RL alone, while maintaining high degree of faithfulness to the expert's decisions, and achieving fast inference with models orders of magnitude smaller and faster than the expert across GymCards, FrozenLake, and BabyAIText suites.

Preliminaries

Behavior Tree (BT) is a hierarchical control structure with a root node and a set of internal control flow nodes and execution (leaf) nodes (Colledanchise and Ögren 2018; Iovino et al. 2022). Control proceeds through a recursive "tick" process starting from the root, with each node returning one of three statuses: SUCCESS, FAILURE, or RUNNING. Control flow nodes determine traversal: a *Sequence* succeeds only if all children succeed, a *Fallback* (or *Selector*) succeeds if any child succeeds, a *Parallel* ticks all children simultaneously and returns SUCCESS or FAILURE once a predefined threshold of children has succeeded or failed, and a *Decorator* modifies the return of its single child (e.g., inverter, repeater, timeout). Execution nodes interact directly with the environment: *Condition* nodes evaluate predicates and return SUCCESS or FAILURE, while *Action* nodes perform operations that may return RUNNING while ongoing and eventually return SUCCESS or FAILURE. Unlike control flow nodes, which are represented by symbolic operators (e.g., $\rightarrow$: *Sequence*, ? : *Selector*, $\rightrightarrows$: *Parallel*), execution nodes are conventionally denoted by shapes, ellipses for conditions and rectangles for actions. This modular, compositional structure makes BTs human readable and reusable, but standard BTs rely on symbolic or hand-engineered condition nodes, limiting their use in high-dimensional perceptual domains such as vision or language.

Imitation learning (IL) seeks to train a policy π that replicates the behavior of an expert π^*, typically from a dataset of demonstrations $\mathcal{D} = \{(s, a)\}$. The simplest form, behavioral cloning (Billard et al. 2008; Argall et al. 2009), treats IL as supervised learning by minimizing prediction loss between π and π^*. However, such offline training suffers from distributional shift: when deployed, the learned policy may visit states not covered in $\mathcal{D}$, compounding errors over time. Iterative IL methods, such as the DAgger (Ross, Gordon, and Bagnell 2011) family of algorithms (Kelly et al. 2019; Hoque et al. 2022; Menda, Driggs-Campbell, and Kochenderfer 2019; Ross and Bagnell 2014), address this issue by collecting expert labels on learner-visited states to mitigate compounding errors. While these methods reduce compounding errors, they require extensive expert queries during training, which can be prohibitively costly in practice.

Reinforcement learning (RL) provides a framework for learning policies through interaction with an environment, typically modeled as a Markov Decision Process (MDP) $\mathcal{M} = (\mathcal{S}, \mathcal{A}, P, R, \gamma)$. Here, $\mathcal{S}$ is the state space, $\mathcal{A}$ the action space, $P(s'|s, a)$ the transition dynamics, $R(s, a)$ the reward function, and $\gamma \in (0, 1)$ the discount factor. A stochastic policy $\pi(a|s)$ defines a distribution over actions given a state, with the objective of maximizing the expected discounted return

$$J(\pi) = \mathbb{E}_{\tau\sim\pi}\left[\sum_{t=0}^{T} \gamma^t r_t\right],$$

where $\tau = (s_0, a_0, \ldots, s_T)$ denotes a trajectory. The policy gradient theorem (Sutton et al. 1999) gives

$$\nabla_\theta J(\pi) = \mathbb{E}_{\tau\sim\pi}[R(\tau)\, \nabla_\theta \log \pi(\tau)],$$

where $R(\tau) = \sum_{t=0}^{T} \gamma^t r_t$ is the trajectory return. In practice, the trajectory return $R(\tau)$ is replaced by variance-reduced estimators such as advantage functions. For example, Generalized Advantage Estimation (GAE) (Schulman et al. 2015) provides a low-variance surrogate that is employed in modern policy optimization methods such as Proximal Policy Optimization (PPO) (Schulman et al. 2017).

Problem Setup

We consider a behavior tree that encodes expert-designed policy for a given task, where condition nodes are expressed in natural language and operate on visual perceptual inputs. Our goal is to train compact models to evaluate these condition nodes so that they remain faithful to an expert's decisions. To achieve that, we assume access to such an expert (or a high-quality expert model, e.g., a large VLM) that can reliably evaluate condition nodes, i.e., judge whether the natural language query associated with each condition node is satisfied by the perceptual input. However, supervision queries are expensive and we have a limited budget for expert supervision. Futhermore, we focus on sparse-reward environments, where feedback is provided only at the end of each episode.

Example 1 (Behavior Tree Execution with Textual Conditions)**.** Figure 1 illustrates a simplified BT for the *BabyAIText Pickup* environment, where condition nodes correspond to natural language queries like *"Is the target object directly in front of the agent?"* or *"Is turning left required to reach the object?"*. At each step during execution, the BT traverses from the root to a leaf and selects a primitive action (e.g., moving forward or rotating). The accuracy of condition-node evaluations on the perceptual inputs determines whether the BT successfully executes the intended policy.

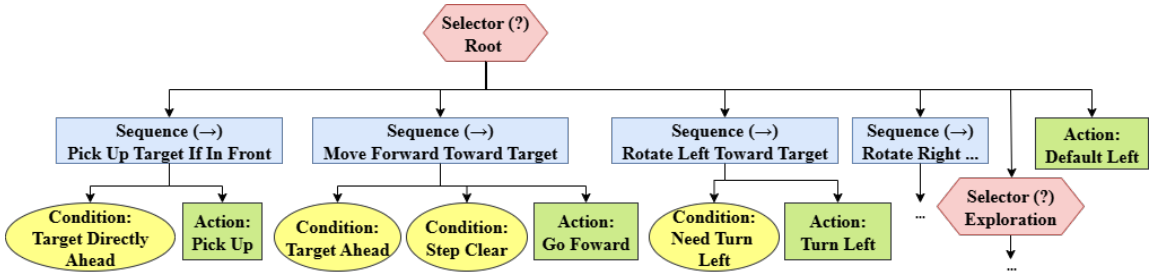

Figure 1: Example behavior tree (BT) for the *BabyAIText Pickup* task. Elliptical leaf nodes represent natural-language condition checks, and rectangular leaf nodes denote primitive actions. Internal control-flow nodes (e.g., Sequence and Selector) determine traversal. The complete tree can be found in the supplementary material.

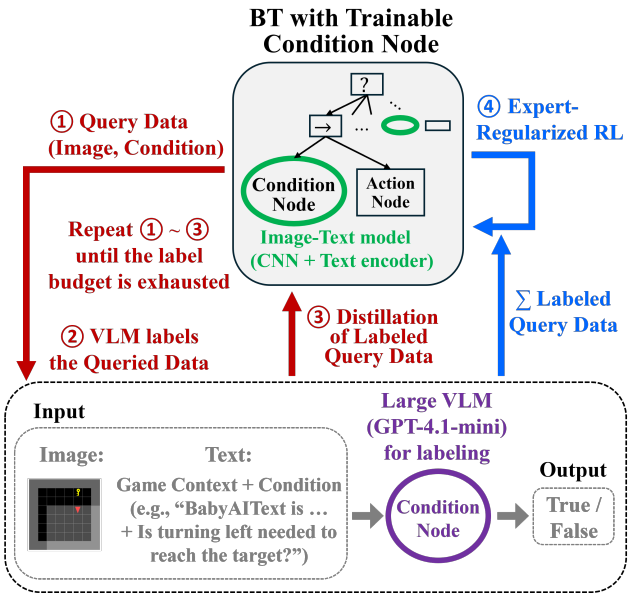

Figure 2: Overview of our framework. The compact model is trained with reinforcement learning under expert regularization, after being initialized with expert labels from a VLM.

Finally, to ensure compatibility with standard MDP formulation, we assume that at each environment step, the BT executes a complete root-to-leaf traversal and produces exactly one primitive action, with no dead ends.

Methodology

We propose a framework that enables lightweight and faithful visual condition checking in BTs via expert-regularized RL (Figure 2). Our approach unifies IL and RL by simultaneously optimizing condition nodes to align with limited expert supervision and to maximize task reward. Expert labels are used for parameter initialization as well as for regularization throughout training, to preserve semantic alignment with expert decisions. At each environment step, the sequence of condition-node decisions is aggregated into a single decision unit corresponding to the chosen action, alleviating the credit assignment challenges described above. This unified process reduces the need for costly expert queries while maintaining faithfulness to expert decisions.

MDP Formulation and Policy Gradient

We formulate the decision-making process under a BT as an MDP $\mathcal{M} = (\mathcal{S}, \mathcal{A}, P, R, \gamma)$, where $\mathcal{S}$ is the state space consisting of high-dimensional perceptual observations (images), $\mathcal{A}$ is the set of primitive actions, $P : \mathcal{S} \times \mathcal{A} \times \mathcal{S} \to [0, 1]$ is the transition function, $R : \mathcal{S} \times \mathcal{A} \to \mathbb{R}$ is the reward function, and γ is the discount factor. We adopt the infinite-horizon discounted formulation ($\gamma \in (0, 1)$) for theoretical clarity, while our experiments are conducted in finite-horizon episodic tasks.

At each step t, the BT $\mathcal{T}$ is traversed from the root to a leaf, producing a sequence of condition-node decisions $\mathbf{y}_t = (y_{t,1}, \ldots, y_{t,n_t})$, where each $y_{t,i} \in \{0, 1\}$ is the binary outcome of the i-th condition node at time t, and n_t is the number of condition nodes evaluated along the traversal. The condition nodes are modeled using a shared binary classifier that receives the current perceptual state s_t (an image) together with the condition node's natural language query q_i. This classifier, implemented as a lightweight neural network, outputs the probability of the decision $y_{t,i}$ given the image–query pair (s_t, q_i), denoted $q_\theta(y_{t,i} \mid s_t, q_i)$, serving as a compact surrogate for the VLM expert. We note that the underlying MDP state space consists solely of images and the queries that represent the condition nodes are part of the fixed BT structure rather than the environment. Importantly, these queries are hand-designed, reflecting the desired behavior for a given task. Given a full decision sequence $\mathbf{y}_t$, it can then be mapped to a primitive action based on the BT.

To formalize this traversal, we use $p(\mathbf{y}_t \mid s_t)$ to denote the probability of selecting the decision sequence $\mathbf{y}_t \in \{0, 1\}^{n_t}$ at a given state $s_t \in \mathcal{S}$. Each sampled sequence $\mathbf{y}_t$ deterministically maps to a primitive action via the BT structure, $\mathcal{T} : \mathcal{Y} \to \mathcal{A}$. The probability distribution p naturally *induces* an action policy, where the probability of selecting an action a_t is given by the sum of probabilities of all decision sequences that map to it:

$$\pi(a_t \mid s_t) = \sum_{\mathbf{y}_t : \mathcal{T}(\mathbf{y}_t) = a_t} p(\mathbf{y}_t \mid s_t). \tag{1}$$

Proposition 1 then shows that this induced policy π is a

valid action distribution, i.e., it is properly normalized and non-negative for all actions $a_t \in \mathcal{A}$.[1]

Proposition 1 (Distribution over Decision Sequences Induces a Valid Action Policy)**.** *Let $p(\mathbf{y}_t \mid s_t)$ be a normalized probability distribution over decision sequences (i.e., $\sum_{\mathbf{y}_t} p(\mathbf{y}_t \mid s_t) = 1$). Assume that the BT $\mathcal{T}$ is deterministic, and for every sequence $\mathbf{y}_t$ with $p(\mathbf{y}_t \mid s_t) > 0$, the BT returns exactly one primitive action $a_t = \mathcal{T}(\mathbf{y}_t) \in \mathcal{A}$. Define the induced action policy*

$$\pi(a_t \mid s_t) \;=\; \sum_{\mathbf{y}_t:\, \mathcal{T}(\mathbf{y}_t)=a_t} p(\mathbf{y}_t \mid s_t). \tag{2}$$

Then $\pi(a_t \mid s_t)$ is a valid probability distribution over $\mathcal{A}$.

While Proposition 1 establishes that the distribution p over decision sequences $\mathbf{y}_t$ induces a valid probability distribution over actions, directly computing $\pi(a_t \mid s_t)$ is inefficient since it requires summing over all decision sequences that map to each action. This issue is especially relevant for policy-gradient optimization, where we need to estimate expectations of functions (e.g., reward or advantage functions) by sampling from the action distribution. Proposition 2 shows that these action-level expectations can instead be written as expectations over the sequence distribution $p(\mathbf{y}_t \mid s_t)$, which will allow us to estimate them by sampling a single root-to-leaf path and using $a_t = \mathcal{T}(\mathbf{y}_t)$, without explicitly forming $\pi(a_t \mid s_t)$.

Proposition 2 (Expectation preservation under deterministic mapping)**.** *Let $a_t = \mathcal{T}(\mathbf{y}_t)$ for a deterministic mapping $\mathcal{T}$, and let $p(\mathbf{y}_t \mid s_t)$ be a valid distribution over decision sequences. Then, for any function f over actions (e.g., reward or advantage functions),*

$$\mathbb{E}_{a_t \sim \pi(\cdot|s_t)}[f(a_t)] = \mathbb{E}_{\mathbf{y}_t \sim p(\cdot|s_t)}[f(\mathcal{T}(\mathbf{y}_t))]. \tag{3}$$

Although Proposition 2 guarantees that expectations over actions can be replaced by expectations over decision sequences $\mathbf{y}_t$, directly modeling the full distribution $p(\mathbf{y}_t \mid s_t)$ is not practical. An autoregressive formulation could in principle capture conditional dependencies across condition nodes, but it would require sequential modeling along the path. This would undermine the reusability property of BTs, namely that condition-node classifiers can be reused across BTs without retraining. Further, it would not be compatible with the form of supervision available from the expert, which provides labels at the node level rather than for entire sequences. Therefore, we adopt a conditional independence assumption, factorizing condition-node decisions as independent given their image–query pairs:

$$p(\mathbf{y}_t \mid s_t) \;=\; \prod_{i=1}^{n_t} q_\theta(y_{t,i} \mid s_t, q_i), \tag{4}$$

where n_t is the number of condition nodes traversed at step t, $y_{t,i} \in \{0, 1\}$ denotes the binary decision at the i-th condition node, and (s_t, q_i) denotes the corresponding image–query pair. Recall that $q_\theta(y_{t,i} \mid s_t, q_i)$ denotes the probability that condition node i outputs $y_{t,i}$ given its image–query input, and it is implemented via a neural classifier parameterized by θ. Consequently, the sequence-level probability p and the action policy π are not parameterized directly, but are instead induced through q_θ and the deterministic BT mapping.

Under the factorization in Eq. (4), an action can be sampled by traversing the BT once from root to leaf, sampling node-level decisions from q_θ and mapping the resulting sequence to a primitive action. This requires evaluating only the nodes encountered along a single traversal, $O(n_{\max})$ per step (where $n_{\max}$ is the maximum depth of the BT), whereas explicitly computing the full action distribution would require aggregating over all possible root-to-leaf decision sequences, whose number can grow exponentially with the tree's branching structure.

Having established both the validity of the induced action distribution (Proposition 1) and the expectation preservation under deterministic mapping (Proposition 2), we now derive the policy gradient under the sequence distribution p, which factorizes into node-level distributions q_θ. Theorem 1 shows that the gradient naturally decomposes into condition-node log-probabilities, making optimization tractable.

Theorem 1 (Policy gradient for BT-driven policies)**.** *Let p denote the distribution over BT decision sequences, which induces the valid action policy π as established in Proposition 1. Using the expectation-preservation property of Proposition 2, the policy gradient is*

$$\nabla_\theta J(\theta) = \mathbb{E}_{\tau \sim \pi}\left[\sum_{t=0}^{T}\sum_{i=1}^{n_t} A_t \, \nabla_\theta \log q_\theta(y_{t,i} \mid s_t, q_i)\right], \tag{5}$$

where A_t is any valid environment-time advantage, and the expectation is over trajectories τ sampled from the environment distribution induced by π.

Importantly, although the policy is factorized over individual condition-node outputs, all condition-node classifiers share a single parameter set θ. At each environment step t, condition nodes along the root-to-leaf path form a grouped decision unit. Specifically, the gradients $\nabla_\theta \log q_\theta(y_{t,i} \mid s_t, q_i)$ for all visited nodes $i = 1, \ldots, n_t$ are accumulated and weighted by the same advantage A_t (Eq. 5), enabling a single parameter update that alleviates credit assignment in sparse-reward settings.

In practice, we optimize a surrogate objective using Proximal Policy Optimization (Schulman et al. 2017), which maximizes the following objective:

$$J_{\mathrm{PPO}}(\theta) = \mathbb{E}_t\left[\min\left(\rho_t(\theta)A_t,\, \mathrm{clip}(\rho_t(\theta), 1-\epsilon, 1+\epsilon)A_t\right)\right], \tag{6}$$

where the importance sampling ratio is defined as

$$\rho_t(\theta) := \frac{\prod_{i=1}^{n_t} q_\theta(y_{t,i} \mid s_t, q_i)}{\prod_{i=1}^{n_t} q_{\theta_{\mathrm{old}}}(y_{t,i} \mid s_t, q_i)}. \tag{7}$$

The advantage estimator A_t is computed using Generalized Advantage Estimation (Schulman et al. 2015). The full PPO loss combines the clipped surrogate in Eq. (6) with the

[1] All proofs appear in the supplementary material.

importance sampling ratio defined over decision sequences (Eq. (7)), plus a value loss based on the state s_t and an entropy bonus computed over the node-level outputs $q_\theta(y_{t,i} \mid s_t, q_i)$, following the standard PPO (Schulman et al. 2017).

Credit assignment under sparse rewards. Our factorized distribution treats all condition-node decisions within an environment step as a single decision sequence $\mathbf{y}_t = (y_{t,1}, \ldots, y_{t,n_t})$ at state s_t, which deterministically induces a primitive action via the BT. The update therefore uses one environment–time advantage A_t attached to the log-probability, $\nabla_\theta \log p(\mathbf{y}_t \mid s_t)\, A_t$. We note that an alternative, simpler MDP formulation could treat each condition-node decision as its own step, with states represented as pairs (s_t, q_i). That is, instead of one environment step t corresponding to a single decision sequence, it is expanded into $(t,1), \ldots, (t,n_t)$ decision states, with the reward only observed after the final decision (t,n_t), which in sparse-reward settings is typically zero until episode termination. This forces credit to propagate backward across $n_t - i$ intra–step links, so the signal available to early decisions (t,i) is geometrically attenuated (approximately $\propto \gamma^{n_t-i}\lambda^{n_t-i}$ with discount γ and GAE parameter λ (Schulman et al. 2015)). By aggregating the intra-step chain, our factorized formulation preserves a concentrated learning signal at the environment timescale and avoids inflating the critic's input domain from s_t to the expanded set of pairs (s_t, q_i) for all traversed condition nodes $i = 1, \ldots, n_t$ at each step, thereby reducing the number of distinct decision states that must be evaluated. In the experiments, we empirically compare our factorized formulation against the simpler baseline.

Expert-Regularized RL Training

RL with Expert Regularization. We optimize the policy via expert-regularized RL, using PPO with Expert Regularization (ER) derived from cross-entropy against expert labels. At each iteration, trajectories are collected by executing the current policy through the BT in the environment. The PPO loss is computed from randomly sampled minibatches, using advantage estimates based on GAE (Schulman et al. 2015) and the importance sampling ratio (Eq. (7)); the value function is simultaneously updated to predict returns, as in standard PPO. To maintain alignment with expert knowledge, we also sample minibatches from the expert dataset $\mathcal{D}_{\text{sup}}$ at every parameter update step and compute the ER loss between the current policy's predictions and the corresponding precomputed VLM labels. The total loss combines the PPO and ER objectives, weighted by a regularization coefficient. The full training procedure is provided in the supplementary material (Algorithm 1).

Imitation Learning Initialization. We initialize the policy using IL. Specifically, we employ either Behavior Cloning (BC) or DAgger under a given labeling budget. For BC, we train on expert-labeled, mission-successful episodes using a cross-entropy loss, with early stopping based on a validation set from an 8:1:1 train/validation/test split; the best checkpoint is then used to initialize RL. For DAgger, we adopt a fixed-budget, chunked aggregation scheme: at each iteration, we (i) collect a fixed quota of new labels by rolling out a mixture policy $\pi_i = \beta_i \pi^* + (1-\beta_i)\hat{\pi}_i$, where π^* is the expert and $\hat{\pi}_i$ is the current learner, with β_i decayed according to an exponential schedule ($\beta_i = \beta_0 \cdot \alpha^i$), and then (ii) perform a single supervised update on the aggregated dataset, using the same cross-entropy objective as in BC. While BC restricts training to successful expert-labeled episodes, DAgger instead aggregates all episodes regardless of outcome, since the mixed policy often has relatively low success rates, resulting in very few successful expert-labeled episodes otherwise. This process is repeated until the total label budget is exhausted, outputting the final dataset $\mathcal{D}_{\text{sup}}$ and the initialized policy π. Notably, BC can be seen as a special case of DAgger where the per-iteration quota equals the entire budget B and the mixture policy is fixed to the expert ($\pi_i = \pi^*$), resulting in a single supervised update. The complete DAgger procedure is provided in the supplementary material (Algorithm 2).

Expert Data Acquisition. To generate expert-labeled data for IL, we deploy the BT in the environment and use a VLM expert to decide whether each condition node is satisfied or not. To do so, we design detailed, game-specific prompts that describe the game context (e.g., mission, rules) and at each condition-decision step, the input – including the rendered image frame, the game context, and the condition query – is provided to the VLM (GPT-4.1-mini), which returns a binary decision. These outputs are collected into a dataset of (image, condition query, decision label) tuples. The resulting expert dataset, $\mathcal{D}_{\text{sup}}$, is then used for both policy initialization and expert regularization during the RL training.

Experiments

Experimental Setup

We evaluate our method on seven distinct visual decision-making tasks drawn from three widely used evaluation suites. These include *NumberLine*, *EZPoints*, and *BlackJack* from GymCards (Zhai et al. 2024); the *4x4* and *8x8* from FrozenLake (Towers et al. 2024); and *Goto* and *Pickup* from BabyAIText (Paglieri et al. 2025). The detailed descriptions of each task are provided in the supplementary material. During training, episodes begin from random initial states to ensure exposure to diverse scenarios, and all experiments are executed with four random seeds. For evaluation, we use a fixed set of 100 episodes generated from four seeds not used in training and report averages over these four seeds.

We report four metrics: (1) *Episodic Success Rate*, the proportion of successful episodes; (2) *Decision Accuracy*, the agreement between the learned model's condition-node decisions and those of the expert VLM (GPT-4.1-mini), measured as the proportion of matching decisions over evaluated samples; (3) *Average Inference Time*, mean runtime per episode; and (4) *Model Size*, the number of parameters in the compact model. Behavior Tree execution uses the `py_trees` (Stonier et al. 2025) library. Expert decisions are obtained from GPT-4.1-mini accessed via API. We allocate a limited budget for each task per random seed: 1,000 VLM queries for *NumberLine* and *FrozenLake 4x4*, and 10,000 VLM queries for *EZPoints*, *BlackJack*, *FrozenLake 8x8*, *BabyAIText Goto*, and *BabyAIText Pickup*. Imple-

Metrics	Model		GymCards			FrozenLake		BabyAIText		
			NL	BJ	EZP	4x4	8x8	Goto	Pickup	Avg
Success Rate (%) ↑	**Expert (GPT-4.1-mini)**		100.00	36.75	78.00	98.25	82.00	99.75	99.50	84.89
	IL	**BC**	**100.00**	40.25	84.50	65.50	13.75	78.75	35.50	59.75
		DA	**100.00**	36.25	44.50	69.75	19.75	66.25	15.75	50.32
	RL	**RL_b**	**100.00**	28.00	0.00	0.00	0.00	5.25	0.75	19.14
		RL_f (ours)	**100.00**	44.00	0.00	97.75	0.00	86.75	2.50	47.29
	IL + RL (ours)	**$init_{BC}$ + RL_f w/ $ER_{1.0}$**	**100.00**	42.50	**89.00**	95.50	58.50	95.25	65.00	77.96
		$init_{BC}$ + RL_f w/ $ER_{0.1}$	**100.00**	44.25	85.00	97.25	66.50	95.50	70.75	**79.89**
	Ablation	**RL_f w/ $ER_{0.1}$**	**100.00**	40.25	0.00	**99.00**	21.75	**98.75**	9.50	52.75
		$init_{BC}$ + RL_f	**100.00**	41.75	78.00	95.00	59.25	95.50	**71.00**	77.21
		$init_{DA}$ + RL_f w/ $ER_{0.1}$	**100.00**	**45.25**	79.00	96.50	**69.25**	93.00	35.25	74.04
Accuracy (%) ↑	**Expert (GPT-4.1-mini)**		100.00	100.00	100.00	100.00	100.00	100.00	100.00	100.00
	IL	**BC**	**100.00**	91.50	98.90	91.54	81.88	83.98	84.67	90.35
		DA	**100.00**	**93.56**	91.85	91.47	**87.09**	83.03	79.74	89.53
	RL	**RL_b**	**100.00**	57.84	53.57	77.78	29.13	69.62	53.75	63.10
		RL_f (ours)	95.71	58.52	61.19	73.09	34.66	76.34	73.05	67.51
	IL + RL (ours)	**$init_{BC}$ + RL_f w/ $ER_{1.0}$**	**100.00**	93.08	**99.21**	**93.45**	82.89	87.07	87.53	**91.89**
		$init_{BC}$ + RL_f w/ $ER_{0.1}$	**100.00**	85.68	98.62	88.59	78.37	**87.33**	**87.94**	89.50
	Ablation	**RL_f w/ $ER_{0.1}$**	**100.00**	75.95	86.00	87.78	76.09	79.77	78.51	83.44
		$init_{BC}$ + RL_f	**100.00**	72.87	95.34	77.44	68.23	84.00	85.49	83.34
		$init_{DA}$ + RL_f w/ $ER_{0.1}$	**100.00**	88.90	97.04	88.48	86.97	87.15	83.00	90.22

Table 1: Performance comparison of models on **Success Rate** and **Accuracy** across seven tasks. Notations: NL = NumberLine, BJ = BlackJack, EZP = EZPoints; BC = Behavior Cloning, DA = DAgger, $\mathbf{RL}_\text{b}$ = baseline RL, $\mathbf{RL}_\text{f}$ = factorized RL, ER = Expert Regularization with coefficients 1.0 and 0.1.

mentation details, including the network architectures, experimental hardware, and hyperparameters, are provided in the supplementary material.

We compare several model variants: **IL baselines**, Behavior Cloning and DAgger; **RL baselines**, the baseline formulation (RL_b), which expands the environment from T steps (episode length in primitive actions) to $K = \sum_{t=1}^{T} n_t$ steps, where n_t is the number of condition nodes traversed at step t, and our factorized formulation (RL_f); **IL+RL**, RL_f with expert regularization, evaluated with regularization coefficients of 1.0 and 0.1; and **Ablations**, variants that remove either initialization or regularization, as well as utilizing alternative initialization based on our Dagger with fixed budget.

Experimental Results

The results are presented in Table 1. Our experiments across the GymCards, FrozenLake, and BabyAIText benchmarks demonstrate that we can successfully learn compact and effective policies that maintain a high level of agreement with the expert. In particular, our integrated CERL framework outperforms both IL and RL baselines individually, while achieving orders-of-magnitude faster inference with a much smaller model size compared to the expert VLM.

CERL Outperforms Baselines. By combining IL and our factorized RL with expert regularization (denoted as $\mathbf{init}_\text{BC}$ + $\mathbf{RL}_\text{f}$ w/ $\mathbf{ER}_{0.1}$), our approach achieves significantly higher success rates than either pure IL (BC or DAgger) or RL alone ($\mathbf{RL}_\text{b}$ baseline or $\mathbf{RL}_\text{f}$ factorized RL). Concretely, the average success rate across all tasks improved to nearly 80% with our IL+RL method compared to around 60% with IL only and less than 50% with factorized RL alone, and only slightly behind the 84.89% of the VLM expert. Furthermore, our factorized RL ($\mathbf{RL}_\text{f}$) consistently outperforms the baseline ($\mathbf{RL}_\text{b}$), improving average success rates from approximately 19% to more than 47%. With a regularization coefficient of 0.1, the model achieves the best balance between reward maximization and semantic fidelity, reaching nearly 80% average success and about 90% accuracy. Notably, using a stronger coefficient ($\mathbf{ER}_{1.0}$) yields further gains in faithfulness: $\mathbf{init}_\text{BC}$ + $\mathbf{RL}_\text{f}$ w/ $\mathbf{ER}_{1.0}$ improves average accuracy from 90.35% (BC) to 91.89%, showing that our approach not only boosts success rates but has the potential to enhance the accuracy of imitation learning itself, further minimizing the gap from the VLM expert. This confirms the effectiveness of our expert-regularized RL in achieving high success rates while preserving strong semantic faithfulness to expert decisions.

Ablation Study Findings. Our ablation analysis validates the contributions of the individual components. Ablating the IL-based initialization ($\mathbf{RL}_\text{f}$ w/ $\mathbf{ER}_{0.1}$) leads to lower accuracy of about 83.4% as well as lower success rate of about 52.8%. Conversely, IL initialization combined with factorized RL but without expert regularization leads to slightly

lower success rate of 77.2% and a more significant decrease in faithfulness. Our proposed framework that consists of IL initialization and expert-regularized RL achieves the best performance across both success rate and accuracy, demonstrating that each component contributes to the overall performance. Additionally, we observe that replacing BC with Dagger ($\mathbf{init}_{\mathrm{DA}} + \mathbf{RL}_{\mathrm{f}}$ w/ $\mathbf{ER}_{0.1}$) tends to underperform compared to BC. This shortfall likely stems from DAgger's limited labeling budget and its mixture policy, which produces fewer successful episodes and thus less effective expert supervision.

Speed, Size, and Cost Efficiency. Our distilled models achieve orders of magnitude faster inference times compared to the expert GPT-4.1-mini VLM, enabling fast execution. Specifically, our IL+RL models infer in approximately 0.09 seconds per episode on average, compared to over 63 seconds for the expert. The compact models we use are significantly smaller than the expert, with approximately 6.6 million parameters versus approximately 7 billion[2](according to estimates), making them several orders of magnitude lighter. Detailed comparisons of speed and model size across all tasks are provided in the supplementary material. Our expert labeling cost was tightly controlled, limited to about 208,000 expert API calls for condition-node decisions across seven tasks and four seeds, corresponding to a total training cost of about US$96.74.

Related Work

A large body of research has combined IL with RL to improve policy performance (Sun, Bagnell, and Boots 2018; Nair et al. 2018; Rajeswaran et al. 2017; Xie et al. 2021; Xue et al. 2023; Song et al. 2023; Ball et al. 2023; Reddy, Dragan, and Levine 2020; Eysenbach, Levine, and Salakhutdinov 2021; Luo et al. 2024). These methods pursue diverse goals, such as surpassing the expert, learning in reward-free settings, or minimizing expert intervention. However, they typically do not emphasize maintaining semantic fidelity to expert behavior or integrating interpretability mechanisms. In contrast, our work leverages IL to preserve faithfulness to expert decisions while using RL for reward optimization, all within an interpretable framework based on BTs.

Although RL has been applied to BTs to improve adaptability and performance, typically by optimizing local node-level decisions such as adjusting fallback priorities (Fu, Qin, and Yin 2016; Zhang et al. 2017; Xu et al. 2022), embedding learned policies into action nodes (Pereira and Engel 2015; Li et al. 2021, 2024), or constructing BT structures through RL-based synthesis (Zhao et al. 2023; Huang et al. 2025), these approaches are largely limited to symbolic or low-dimensional feature spaces as RL inputs. This limitation restricts their applicability to high-dimensional perceptual inputs such as images and language without costly feature engineering. In addition, many of these methods modify or replace standard BT nodes, for example, by embedding opaque neural policies into action nodes or altering control-flow logic, thereby weakening alignment with the human designer's intent and reducing the transparency and interpretability that BTs are meant to provide. In contrast, our approach preserves the standard BT structure by keeping action and control-flow nodes unchanged, while training only condition nodes with lightweight neural models regularized by expert supervision to retain their intended semantics.

Decision trees (Breiman et al. 2017) have also been explored as interpretable policy representations in RL. Prior studies primarily fall into two directions. Distillation-based methods extract tree policies from trained RL agents to enhance transparency and verifiability (Bastani, Pu, and Solar-Lezama 2018; Acero and Li 2024), while differentiable methods learn tree parameters end-to-end through gradient-based optimization (Silva et al. 2020; Wen et al. 2025). To our knowledge, no prior approach has introduced a factorized policy formulation that enables efficient root-to-leaf sampling-based policy-gradient optimization for differentiable tree structures, nor has it enabled direct training of expert-designed, tree-structured policies from high-dimensional perceptual inputs for sequential decision-making.

Conclusion

We presented a unified framework for interpretable sequential decision-making based on expert-designed behavior trees that operate on high-dimensional perceptual inputs, integrating imitation learning and reinforcement learning through expert regularization. Our approach uses a limited set of expert labels, leveraging them both for initialization and as a continuous regularizer to preserve semantic alignment with expert decisions. Reinforcement learning drives performance improvement, while expert regularization constrains the policy to remain close to expert behavior. The RL component is built on factorized node-level distributions that aggregate condition-node decisions into a single unit, simplifying credit assignment under sparse rewards. Across the GymCards, FrozenLake, and BabyAIText suites, we showed that our approach achieves strong success rates, maintains semantic consistency with expert behavior, and runs efficiently on lightweight models suitable for resource-constrained environments.

Our work focuses on expert-designed BTs that encode agents' desired policies for successfully completing tasks while operating on high-dimensional perceptual inputs. It assumes access to an expert model (e.g., VLM) that is capable of judging natural-language queries over perceptual inputs with high accuracy, but incurs high computational costs. In future work, we plan to extend our work to consider additional settings such as automated BT synthesis and adaptation, or the use of weaker or noisier supervision sources in place of strong expert models.

Acknowledgments

This research was supported by grant number DSI-CGY3R1P18 from the Data Sciences Institute at the University of Toronto. The authors also gratefully acknowledge funding from the Natural Sciences and Engineering Research Council of Canada (NSERC).

[2]Unofficial estimate, e.g., https://amigochat.io/gpt-4-1-mini

References

Acero, F.; and Li, Z. 2024. Distilling reinforcement learning policies for interpretable robot locomotion: Gradient boosting machines and symbolic regression. In *Proceedings of the IEEE/RSJ International Conference on Intelligent Robots and Systems (IROS)*, 6840–6847. IEEE.

Argall, B. D.; Chernova, S.; Veloso, M.; and Browning, B. 2009. A survey of robot learning from demonstration. *Robotics and Autonomous Systems*, 57(5): 469–483.

Ball, P. J.; Smith, L.; Kostrikov, I.; and Levine, S. 2023. Efficient online reinforcement learning with offline data. In *Proceedings of the 40th International Conference on Machine Learning (ICML)*, 1577–1594. PMLR.

Bastani, O.; Pu, Y.; and Solar-Lezama, A. 2018. Verifiable reinforcement learning via policy extraction. 31.

Billard, A.; Calinon, S.; Dillmann, R.; and Schaal, S. 2008. Robot programming by demonstration. In *Springer Handbook of Robotics*, 1371–1394. Springer.

Breiman, L.; Friedman, J.; Olshen, R. A.; and Stone, C. J. 2017. *Classification and regression trees*. Chapman and Hall/CRC.

Colledanchise, M.; and Ögren, P. 2018. *Behavior trees in robotics and AI: an introduction*. CRC Press.

Colledanchise, M.; Parasuraman, R.; and Ögren, P. 2018. Learning of behavior trees for autonomous agents. *IEEE Transactions on Games*, 11(2): 183–189.

Eysenbach, B.; Levine, S.; and Salakhutdinov, R. R. 2021. Replacing rewards with examples: example-based policy search via recursive classification. *Advances in Neural Information Processing Systems*, 34: 11541–11552.

Fu, Y.; Qin, L.; and Yin, Q. 2016. A reinforcement learning behavior tree framework for game AI. In *2016 International Conference on Economics, Social Science, Arts, Education and Management Engineering*, 573–579. Atlantis Press.

Ghosh, A.; Acharya, A.; Saha, S.; Jain, V.; and Chadha, A. 2024. Exploring the frontier of vision-language models: a survey of current methodologies and future directions. *CoRR*.

Ghzouli, R.; Berger, T.; Johnsen, E. B.; Dragule, S.; and Wasowski, A. 2020. Behavior trees in action: a study of robotics applications. In *Proceedings of the 13th ACM SIGPLAN International Conference on Software Language Engineering*, 196–209. ACM.

Hoque, R.; Balakrishna, A.; Novoseller, E.; Wilcox, A.; Brown, D. S.; and Goldberg, K. 2022. ThriftyDAgger: budget-aware novelty and risk gating for interactive imitation learning. In *Proceedings of the 5th Conference on Robot Learning (CoRL)*, 598–608. PMLR.

Hu, H.; Jia, X.; Liu, K.; and Sun, B. 2021. Self-Adaptive traffic control model with behavior trees and reinforcement learning for AGV in industry 4.0. *IEEE Transactions on Industrial Informatics*, 17(12): 7968–7979.

Huang, Y.; Wu, Z.; Ma, K.; and Wang, J. 2025. Differentiable synthesis of behavior tree architectures and execution nodes. In *Proceedings of the 2nd International Conference on Neuro-Symbolic Systems (NeuS 2025)*, volume 288. PMLR.

Iovino, M.; Scukins, E.; Styrud, J.; Ögren, P.; and Smith, C. 2022. A survey of behavior trees in robotics and AI. *Robotics and Autonomous Systems*, 154: 104096.

Kelly, M.; Sidrane, C.; Driggs-Campbell, K.; and Kochenderfer, M. J. 2019. HG-DAgger: interactive imitation learning with human experts. In *Proceedings of the IEEE International Conference on Robotics and Automation (ICRA)*, 8077–8083. IEEE.

Li, L.; Wang, L.; Li, Y.; and Sheng, J. 2021. Mixed deep reinforcement learning–behavior tree for intelligent agents design. In *Proceedings of the 13th International Conference on Agents and Artificial Intelligence (ICAART)*, 113–124.

Li, X.; Li, Y.; Zhang, J.; Xu, X.; and Liu, D. 2024. Embedding multi-agent reinforcement learning into behavior trees with unexpected interruptions. *Complex & Intelligent Systems*, 10(3): 3273–3282.

Luo, J.; Dong, P.; Zhai, Y.; Ma, Y.; and Levine, S. 2024. RLIF: interactive imitation learning as reinforcement learning. In *Proceedings of the 12th International Conference on Learning Representations (ICLR)*.

Marcotte, R.; and Hamilton, H. J. 2017. Behavior trees for modelling artificial intelligence in games: a tutorial. *The Computer Games Journal*, 6(3): 171–184.

Menda, K.; Driggs-Campbell, K.; and Kochenderfer, M. J. 2019. EnsembleDAgger: a bayesian approach to safe imitation learning. In *Proceedings of the IEEE/RSJ International Conference on Intelligent Robots and Systems (IROS)*, 5041–5048. IEEE.

Nair, A.; McGrew, B.; Andrychowicz, M.; Zaremba, W.; and Abbeel, P. 2018. Overcoming exploration in reinforcement learning with demonstrations. In *Proceedings of the IEEE International Conference on Robotics and Automation (ICRA)*, 6292–6299. IEEE.

Ögren, P.; and Sprague, C. I. 2022. Behavior trees in robot control systems. *Annual Review of Control, Robotics, and Autonomous Systems*, 5(1): 81–107.

Paglieri, D.; Cupiał, B.; Coward, S.; Piterbarg, U.; Wolczyk, M.; Khan, A.; Pignatelli, E.; Kuciński, Ł.; Pinto, L.; Fergus, R.; et al. 2025. BALROG: benchmarking agentic LLM and VLM reasoning on games. In *Proceedings of the 13th International Conference on Learning Representations (ICLR)*.

Pereira, R. d. P.; and Engel, P. M. 2015. A framework for constrained and adaptive behavior-based agents. *arXiv preprint arXiv:1506.02312*.

Rajeswaran, A.; Kumar, V.; Gupta, A.; Vezzani, G.; Schulman, J.; Todorov, E.; and Levine, S. 2017. Learning complex dexterous manipulation with deep reinforcement learning and demonstrations. *arXiv preprint arXiv:1709.10087*.

Reddy, S.; Dragan, A. D.; and Levine, S. 2020. SQIL: imitation learning via reinforcement learning with sparse rewards. In *Proceedings of the 8th International Conference on Learning Representations (ICLR)*.

Ross, S.; and Bagnell, J. A. 2014. Reinforcement and imitation learning via interactive no-regret learning. *arXiv preprint arXiv:1406.5979*.

Ross, S.; Gordon, G.; and Bagnell, D. 2011. A reduction of imitation learning and structured prediction to no-regret online learning. In *Proceedings of the 14th International Conference on Artificial Intelligence and Statistics (AISTATS)*, 627–635. JMLR Workshop and Conference Proceedings.

Schulman, J.; Moritz, P.; Levine, S.; Jordan, M.; and Abbeel, P. 2015. High-Dimensional continuous control using generalized advantage estimation. *arXiv preprint arXiv:1506.02438*.

Schulman, J.; Wolski, F.; Dhariwal, P.; Radford, A.; and Klimov, O. 2017. Proximal policy optimization algorithms. *arXiv preprint arXiv:1707.06347*.

Silva, A.; Killian, T.; Jimenez, I.; Son, S.-H.; and Gombolay, M. 2020. Optimization methods for interpretable differentiable decision trees applied to reinforcement learning. In *Proceedings of the 23th International Conference on Artificial Intelligence and Statistics (AISTATS)*, 1855–1865. PMLR.

Skalse, J.; Howe, N.; Krasheninnikov, D.; and Krueger, D. 2022. Defining and characterizing reward gaming. *Advances in Neural Information Processing Systems*, 35: 9460–9471.

Song, Y.; Zhou, Y.; Sekhari, A.; Bagnell, D.; Krishnamurthy, A.; and Sun, W. 2023. Hybrid RL: using both offline and online data can make RL efficient. In *Proceedings of the 11th International Conference on Learning Representations (ICLR)*.

Stonier, D.; et al. 2025. py_trees: Pythonic Behaviour Trees for Python. https://github.com/splintered-reality/py_trees.

Sun, W.; Bagnell, J. A.; and Boots, B. 2018. Truncated horizon policy search: combining reinforcement learning & imitation learning. In *Proceedings of the 6th International Conference on Learning Representations (ICLR)*.

Sutton, R. S.; McAllester, D.; Singh, S.; and Mansour, Y. 1999. Policy gradient methods for reinforcement learning with function approximation. In *Advances in Neural Information Processing Systems*, volume 12. MIT Press.

Towers, M.; Kwiatkowski, A.; Terry, J.; Balis, J. U.; De Cola, G.; Deleu, T.; Goulao, M.; Kallinteris, A.; Krimmel, M.; KG, A.; et al. 2024. Gymnasium: a standard interface for reinforcement learning environments. *arXiv preprint arXiv:2407.17032*.

Wake, N.; Kanehira, A.; Takamatsu, J.; Sasabuchi, K.; and Ikeuchi, K. 2025. VLM-Driven behavior tree for context-aware task planning. *arXiv preprint arXiv:2501.03968*.

Wen, Y.; Li, S.; Zuo, R.; Yuan, L.; Mao, H.; and Liu, P. 2025. SkillTree: Explainable Skill-Based Deep Reinforcement Learning for Long-Horizon Control Tasks. In *Proceedings of the AAAI Conference on Artificial Intelligence*, volume 39, 21491–21500.

Williams, R. J. 1992. Simple statistical gradient-following algorithms for connectionist reinforcement learning. *Machine Learning*, 8: 229–256.

Xie, T.; Jiang, N.; Wang, H.; Xiong, C.; and Bai, Y. 2021. Policy finetuning: bridging sample-efficient offline and online reinforcement learning. *Advances in Neural Information Processing Systems*, 34: 27395–27407.

Xu, J.; Lin, Y.; Zhou, H.; and Min, H. 2022. Generating manipulation sequences using reinforcement learning and behavior trees for peg-in-hole task. In *Proceedings of the IEEE International Conference on Systems, Man, and Cybernetics (SMC)*, 2715–2720. IEEE.

Xue, Z.; Peng, Z.; Li, Q.; Liu, Z.; and Zhou, B. 2023. Guarded policy optimization with imperfect online demonstrations. *arXiv preprint arXiv:2303.01728*.

Zare, M.; Kebria, P. M.; Khosravi, A.; and Nahavandi, S. 2024. A survey of imitation learning: algorithms, recent developments, and challenges. *IEEE Transactions on Cybernetics*.

Zhai, S.; Bai, H.; Lin, Z.; Pan, J.; Tong, P.; Zhou, Y.; Suhr, A.; Xie, S.; LeCun, Y.; Ma, Y.; et al. 2024. Fine-Tuning large vision-language models as decision-making agents via reinforcement learning. *Advances in Neural Information Processing Systems*, 37: 110935–110971.

Zhang, Q.; Sun, L.; Jiao, P.; and Yin, Q. 2017. Combining behavior trees with MAXQ learning to facilitate CGFs behavior. In *Proceedings of the 4th International Conference on Systems and Informatics (ICSAI)*, 525–531. IEEE.

Zhao, C.; Deng, C.; Liu, Z.; Zhang, J.; Wu, Y.; Wang, Y.; and Yi, X. 2023. Interpretable reinforcement learning of behavior trees. In *Proceedings of the 15th International Conference on Machine Learning and Computing*, 492–499.

Supplementary Materials

Proofs

This section provides detailed proofs for the key theoretical results presented in the main paper.

Proposition 1. (Distribution over Decision Sequences Induces a Valid Action Policy) *Let $p(\mathbf{y}_t \mid s_t)$ be a normalized probability distribution over decision sequences (i.e., $\sum_{\mathbf{y}_t} p(\mathbf{y}_t \mid s_t) = 1$). Assume that the BT $\mathcal{T}$ is deterministic, and for every sequence $\mathbf{y}_t$ with $p(\mathbf{y}_t \mid s_t) > 0$, the BT returns exactly one primitive action $a_t = \mathcal{T}(\mathbf{y}_t) \in \mathcal{A}$. Define the induced action policy*

$$\pi(a_t \mid s_t) \;=\; \sum_{\mathbf{y}_t:\, \mathcal{T}(\mathbf{y}_t)=a_t} p(\mathbf{y}_t \mid s_t). \tag{8}$$

Then $\pi(a_t \mid s_t)$ is a valid probability distribution over $\mathcal{A}$.

Proof. Each term $p(\mathbf{y}_t \mid s_t)$ is nonnegative, so $\pi(a_t \mid s_t) \geq 0$ for every $a_t \in \mathcal{A}$. To show the probabilities over actions sum to 1, add them up:

$$\sum_{a_t \in \mathcal{A}} \pi(a_t \mid s_t) = \sum_{a_t \in \mathcal{A}} \sum_{\mathbf{y}_t:\, \mathcal{T}(\mathbf{y}_t)=a_t} p(\mathbf{y}_t \mid s_t). \tag{9}$$

Because the BT is deterministic, each sequence that can occur (i.e., has $p(\mathbf{y}_t \mid s_t) > 0$) leads to exactly one action, so each sequence $\mathbf{y}_t$ appears in exactly one of the inner sums. Sequences with zero probability do not contribute. Therefore the double sum counts each occurring sequence exactly once, giving

$$\sum_{a_t \in \mathcal{A}} \pi(a_t \mid s_t) = \sum_{\mathbf{y}_t} p(\mathbf{y}_t \mid s_t) = 1. \tag{10}$$

Thus $\pi(a_t \mid s_t)$ is nonnegative and sums to 1, so it is a valid probability distribution over $\mathcal{A}$. □

Proposition 2. (Expectation preservation under deterministic mapping) *Let $a_t = \mathcal{T}(\mathbf{y}_t)$ for a deterministic mapping $\mathcal{T}$, and let $p(\mathbf{y}_t \mid s_t)$ be a valid distribution over decision sequences. Then, for any function f over actions (e.g., reward or advantage functions),*

$$\mathbb{E}_{a_t \sim \pi(\cdot|s_t)}[f(a_t)] = \mathbb{E}_{\mathbf{y}_t \sim p(\cdot|s_t)}[f(\mathcal{T}(\mathbf{y}_t))]. \tag{11}$$

Proof. By the law of total probability (Proposition 1, Eq. (8)),

$$\mathbb{E}_{a_t \sim \pi(\cdot|s_t)}[f(a_t)] = \sum_{a_t} \pi(a_t \mid s_t) f(a_t) \tag{12}$$

$$= \sum_{a_t} \left(\sum_{\mathbf{y}_t : \mathcal{T}(\mathbf{y}_t) = a_t} p(\mathbf{y}_t \mid s_t) \right) f(a_t) \tag{13}$$

$$= \sum_{\mathbf{y}_t} p(\mathbf{y}_t \mid s_t) f(\mathcal{T}(\mathbf{y}_t)) \tag{14}$$

$$= \mathbb{E}_{\mathbf{y}_t \sim p(\cdot|s_t)}[f(\mathcal{T}(\mathbf{y}_t))]. \tag{15}$$

The crucial step is the move from Eq. (13) to Eq. (14). Since each sequence $\mathbf{y}_t$ deterministically maps to exactly one action $a_t = \mathcal{T}(\mathbf{y}_t)$, Eq. (13) becomes equivalent to summing once over all sequences and evaluating f at the induced action $\mathcal{T}(\mathbf{y}_t)$. □

Theorem 1. (Policy gradient for BT-driven policies) *Let p denote the distribution over BT decision sequences, which induces the valid action policy π as established in Proposition 1. Using the expectation-preservation property of Proposition 2, the policy gradient is*

$$\nabla_\theta J(\theta) = \mathbb{E}_{\tau \sim \pi} \left[\sum_{t=0}^{T} \sum_{i=1}^{n_t} A_t \, \nabla_\theta \log q_\theta(y_{t,i} \mid s_t, q_i) \right], \tag{16}$$

where A_t is any valid environment-time advantage, and the expectation is over trajectories τ sampled from the environment distribution induced by π.

Proof. We define the RL environment as a Markov Decision Process, $\mathcal{M} = (\mathcal{S}, \mathcal{A}, P, R, \gamma)$. Let $\tau = (s_0, \mathbf{y}_0, a_0, r_0, s_1, \ldots, s_{T+1})$ denote a trajectory. Its probability under the induced action policy π is given by

$$\pi(\tau) = p_0(s_0) \prod_{t=0}^{T} \left[\pi(a_t \mid s_t) \; P(s_{t+1} \mid s_t, a_t) \right] \tag{17}$$

$$= p_0(s_0) \prod_{t=0}^{T} \left[p(\mathbf{y}_t \mid s_t) \; P(s_{t+1} \mid s_t, a_t) \right] \tag{18}$$

$$= p_0(s_0) \prod_{t=0}^{T} \left[\prod_{i=1}^{n_t} q_\theta(y_{t,i} \mid s_t, q_i) \; P(s_{t+1} \mid s_t, a_t) \right], \tag{19}$$

where $p_0(\cdot)$ is the initial state distribution.

By the log-derivative trick (Sutton et al. 1999; Williams 1992), for any differentiable policy,

$$\nabla_\theta J(\theta) = \nabla_\theta \mathbb{E}_{\tau \sim \pi}[R(\tau)] = \mathbb{E}_{\tau \sim \pi} \left[R(\tau) \, \nabla_\theta \log \pi(\tau) \right]. \tag{20}$$

The full trajectory log-probability is

$$\log \pi(\tau) = \log p_0(s_0) + \sum_{t=0}^{T} \sum_{i=1}^{n_t} \log q_\theta(y_{t,i} \mid s_t, q_i) \tag{21}$$

$$+ \sum_{t=0}^{T} \log P(s_{t+1} \mid s_t, a_t). \tag{22}$$

The initial state distribution p_0 and the transition probability distribution P do not depend on θ, so their gradient vanishes. Thus,

$$\nabla_\theta \log \pi(\tau) = \sum_{t=0}^{T} \sum_{i=1}^{n_t} \nabla_\theta \log q_\theta(y_{t,i} \mid s_t, q_i), \tag{23}$$

substituting $\nabla_\theta \log \pi(\tau)$ into the expectation, and using that the return $R(\tau)$ can be replaced by an advantage-weighted sum without changing the expectation, we obtain

$$\nabla_\theta J(\theta) \;=\; \mathbb{E}_{\tau \sim \pi} \left[\sum_{t=0}^{T} \sum_{i=1}^{n_t} A_t \; \nabla_\theta \log q_\theta\big(y_{t,i} \mid s_t, q_i\big) \right]. \tag{24}$$

□

In practice, we optimize a surrogate objective using Proximal Policy Optimization (Schulman et al. 2017), which maximizes the following objective:

$$J_{\mathrm{PPO}}(\theta) = \mathbb{E}_t \left[\min \left(\rho_t(\theta) A_t, \; \mathrm{clip}(\rho_t(\theta), 1 - \epsilon, 1 + \epsilon) A_t \right) \right], \tag{25}$$

where the importance sampling ratio is defined as

$$\rho_t(\theta) := \frac{\prod_{i=1}^{n_t} q_\theta(y_{t,i} \mid s_t, q_i)}{\prod_{i=1}^{n_t} q_{\theta_{\mathrm{old}}}(y_{t,i} \mid s_t, q_i)}. \tag{26}$$

The advantage estimator A_t is computed using Generalized Advantage Estimation (Schulman et al. 2015). The full PPO loss combines the clipped surrogate in Eq. (25) with the importance sampling ratio defined over decision sequences (Eq. (26)), plus a value loss based on the state s_t and an entropy bonus computed over the node-level outputs $q_\theta(y_{t,i} \mid s_t, q_i)$, following the standard PPO (Schulman et al. 2017).

Algorithms

This section presents the complete pseudocode for the algorithms discussed in the main paper, including CERL (Condition-node Expert-Regularized Reinforcement Learning) and DAgger with Fixed Label Budget. These implementations correspond to Algorithms 1 and 2 referenced in the main text.

Metrics	Model		GymCards			FrozenLake		BabyAIText		Avg
			NL	BJ	EZP	4x4	8x8	Goto	Pickup	
Inference Time (s/ep) ↓	Expert (GPT-4.1-mini)		4.82	13.24	39.58	60.18	241.51	31.86	52.54	63.39
	IL	BC	**0.01**	0.17	0.08	0.03	**0.06**	0.09	0.37	0.12
		DA	**0.01**	0.17	0.07	0.05	0.28	0.14	0.46	0.17
	RL	$\mathbf{RL}_{\text{b}}$	**0.01**	**0.15**	**0.05**	0.28	1.53	0.42	0.35	0.40
		$\mathbf{RL}_{\text{f}}$ **(ours)**	**0.01**	0.16	0.14	**0.02**	0.72	0.09	0.35	0.21
	IL + RL (ours)	init_{BC} + $\mathbf{RL}_{\text{f}}$ w/ $\mathbf{ER}_{1.0}$	**0.01**	0.17	0.11	0.04	0.11	0.07	0.16	**0.09**
		init_{BC} + $\mathbf{RL}_{\text{f}}$ w/ $\mathbf{ER}_{0.1}$	**0.01**	0.17	0.11	0.03	0.14	0.06	**0.11**	**0.09**
	Ablation	$\mathbf{RL}_{\text{f}}$ w/ $\mathbf{ER}_{0.1}$	**0.01**	**0.15**	0.08	**0.02**	0.11	**0.03**	0.42	0.12
		init_{BC} + $\mathbf{RL}_{\text{f}}$	**0.01**	0.17	0.12	0.04	0.19	0.06	0.16	0.11
		init_{DA} + $\mathbf{RL}_{\text{f}}$ w/ $\mathbf{ER}_{0.1}$	**0.01**	0.16	0.12	0.03	0.36	0.11	0.43	0.18
Model Size (# params) ↓	Expert (GPT-4.1-mini)		∼7B[3]							
	Others		6.6M							

Table 2: Inference time and model size across seven tasks. NL = NumberLine, BJ = BlackJack, EZP = EZPoints; BC = Behavior Cloning, DA = DAgger, $\mathbf{RL}_{\text{b}}$ = baseline RL, $\mathbf{RL}_{\text{f}}$ = factorized RL, ER = Expert Regularization (coefficients 1.0 and 0.1).

Algorithm 1: CERL: Condition-node Expert-regularized Reinforcement Learning

Input: Behavior Tree $\mathcal{T}$, initial policy π (parameters θ), environment $\mathcal{E}$, expert dataset $\mathcal{D}_{\text{sup}}$, expert-regularization (ER) coefficient λ_{ER}
Output: policy π

Initialize π on $\mathcal{D}_{\text{sup}}$ via imitation learning (e.g., Behavior Cloning or DAgger - Algorithm 2)
for each iteration **do**
  Collect trajectories $\mathcal{D}$ in $\mathcal{E}$ using BT $\mathcal{T}$ and policy π
  Compute returns and advantages (GAE) from $\mathcal{D}$
  for each PPO epoch **do**
    for each minibatch $(\mathbf{S}, \mathbf{Y}, \mathbf{A}, R, \hat{A})$ in $\mathcal{D}$ **do**
      Compute L_{PPO}: PPO loss based on importance ratio Eq. (26), including value and entropy terms
      Sample minibatch $(\mathbf{S}_{\text{sup}}, \mathbf{Q}_{\text{sup}}, \mathbf{Y}_{\text{sup}})$ from $\mathcal{D}_{\text{sup}}$
      Compute L_{ER}: averaged cross-entropy loss between $\pi(y_{\text{sup}} \mid s_{\text{sup}}, q_{\text{sup}})$ and expert labels y_{sup}
      Update θ to minimize $L_{\text{PPO}} + \lambda_{\text{ER}} L_{\text{ER}}$
return π_θ

Algorithm 2: DAgger with Fixed Label Budget

Input: Behavior Tree $\mathcal{T}$, environment $\mathcal{E}$, expert policy π^*, initial policy π (parameters θ), total budget B, per-iteration quota q, initial mix β_0, decay $\alpha \in (0, 1)$
Output: Aggregated dataset $\mathcal{D}_{\text{sup}}$, policy π
Notation: $x = (\text{image}, \text{condition query})$ for learner input; $x^+ = (\text{image}, \text{game context} + \text{condition query})$ for expert input

$\hat{\pi}_0 \leftarrow \pi$; $\mathcal{D}_{\text{sup}} \leftarrow \emptyset$; $b \leftarrow B$; $i \leftarrow 0$
while $b > 0$ **do**
  $\beta_i \leftarrow \min\{1, \beta_0 \alpha^i\}$; $c \leftarrow \min\{q, b\}$
  Define rollout mixture: $\pi_i = \beta_i \pi^* + (1 - \beta_i)\, \hat{\pi}_i$
  while $c > 0$ **do**
    Roll out $\mathcal{T}$ for one tick in $\mathcal{E}$ using π_i
    Get $D_i = \{(x, \pi^*(x^+))\}$ of condition queries visited by π_i
    $\mathcal{D}_{\text{sup}} \leftarrow \mathcal{D}_{\text{sup}} \cup D_i$; $c \leftarrow c - |D_i|$; $b \leftarrow b - |D_i|$
  Update $\hat{\pi}_i$ on $\mathcal{D}_{\text{sup}}$ with cross-entropy
  $i \leftarrow i + 1$
$\pi \leftarrow \hat{\pi}_i$
return $(\mathcal{D}_{\text{sup}}, \pi)$

Extended and Additional Experimental Results

Speed and Model Size. As shown in Table 2, our compact models demonstrate significant advantages in both inference speed and size compared to the expert GPT-4.1-mini VLM. Across all tasks, the distilled IL+RL variants achieve average inference times of roughly 0.09 seconds per episode, while the expert requires more than 63 seconds on average. This efficiency gain corresponds to a speedup of over three orders of magnitude. In terms of size, each compact model contains approximately 6.6 million parameters, compared to the expert's estimated 7 billion, making our approach both computationally and memory efficient.

Effect of Expert Data Size. To evaluate the impact of expert dataset size, we train models using behavior cloning with $0.5 \times 10{,}000$ and $0.2 \times 10{,}000$ expert labels on the *FrozenLake 8x8* and *BabyAIText Pickup* tasks, averaging results over four random seeds. As shown in Figure 3, reducing the amount of expert-labeled data leads to a clear decline in both success rate and accuracy.

Experimental Details

Model Architectures. We implemented two variants of the actor–critic network for condition-node policies: our

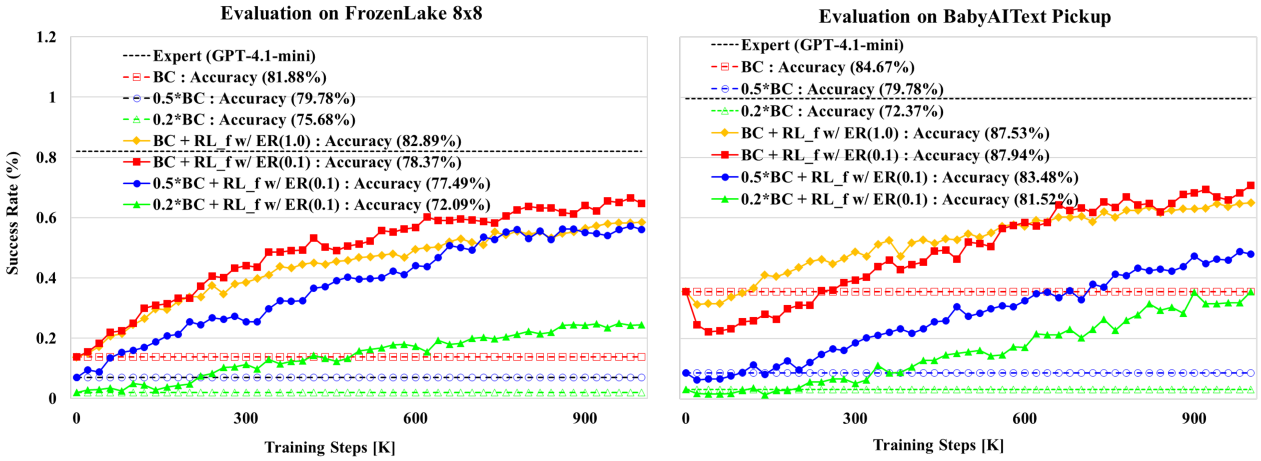

Figure 3: Effect of expert dataset size on *FrozenLake 8x8* (left) and *BabyAIText Pickup* (right). While expert-regularized RL improves performance even with limited expert labels, models trained with fewer labels (0.5× and 0.2× of the full dataset) show progressively lower success rates and reduced agreement with expert decisions (accuracy), underscoring the need for minimal expert supervision for overall performance. Results are averaged over four random seeds.

proposed factorized RL (**RL$_\mathbf{f}$**) and the baseline RL (**RL$_\mathbf{b}$**). Both share the same image and text encoder architecture but differ in how the critic's state representation is defined. The detailed architectures are provided in Table 3 and Table 4.

In the factorized formulation (**RL**$_\text{f}$), the environment state at step t is defined as $s_t = \text{image}_t$. Each condition-node query (e.g., a sentence) is mapped to a token in the vocabulary, with identical queries sharing the same token id and embedding. The text encoder retrieves a single embedding vector for the query token, which is combined with the image feature by the actor to produce condition decisions. The critic, however, depends only on the image feature and computes $V(s_t)$, reducing the critic's input domain.

In the baseline setting (**RL**$_\text{b}$), each condition decision (t, i) is treated as a separate state $s_{t,i} = (\text{image}_t, \text{text}_{t,i})$, where $\text{text}_{t,i}$ is the query associated with condition node i. Queries are again mapped to vocabulary tokens, with identical queries sharing the same token id and embedding. The text encoder retrieves the query embedding, which the actor combines with the image feature to produce condition decisions. Unlike **RL**$_\text{f}$, the critic also takes the query into account, computing $V(s_{t,i})$ from the joint image–text input. This enlarges the critic's input domain and complicates credit assignment under sparse rewards.

Computing Environment. All experiments run on a Windows 11 workstation with Intel 64-bit CPU @2.0GHz, 32GB RAM, and NVIDIA GeForce RTX 4090 GPU 24GB. Behavior Tree execution is implemented using the `py_trees` (Stonier et al. 2025) library.

Hyperparameters. The principal hyperparameters used for training and evaluation are summarized in Table 5. These include model parameters, optimization settings, RL-specific coefficients, supervised learning configurations, evaluation, and expert parameters.

Experimental Environments

GymCards. We evaluate our method on visual reasoning and decision-making tasks from the GymCards suite (Zhai et al. 2024): *NumberLine*, *EZPoints*, and *BlackJack*. In *NumberLine*, the agent operates in a deterministic environment and must increment or decrement a visual counter to match a target number, requiring basic numeric comparison. *EZPoints* is a visual arithmetic task in which the agent is shown two playing cards, each displaying a number, and must use arithmetic operators to build an expression that equals a fixed target value (e.g., 12); each card is used once, demanding both visual perception and symbolic reasoning. *BlackJack* is a stochastic version of the classic card game, where the agent decides whether to "hit" or "stand" based on visually observed cards, with uncertainty introduced by hidden cards and random draws. Figure 5 illustrates a step-by-step progression in *EZPoints*.

FrozenLake. We assess our approach on two visual navigation tasks based on the classic FrozenLake environment in *4x4* and *8x8* random grid settings (Towers et al. 2024). In each episode, the agent is presented with a top-down grid map and must navigate from a start position to a designated goal, avoiding "holes" that terminate the episode. The environment is fully observable and deterministic, but the larger *8x8* grid increases task complexity by introducing a greater number of possible paths and obstacles. Both variants require spatial reasoning and safe action selection, with the *8x8* setting posing a significantly greater challenge in terms of path diversity and episode length, under the sparse-reward settings described earlier.

[3]Unofficial estimate, e.g., https://amigochat.io/gpt-4-1-mini

Component	Layer	Output dim.
Image encoder	Conv2d(3, 64, 3×3, 3) + ReLU Conv2d(64, 64, 3×3, 1) + ReLU Flatten + Linear(d_{flatten}, 64)	d_{img}=64
Text encoder	Embedding ($\|token\|$, $d_{\text{emb}} = 32$) → Linear(32, 32)	d_{text}=32
Actor	Linear($d_{\text{img}} + d_{\text{text}}$, 64) + ReLU → Linear(64, 2)	logits (Success/Failure)=2
Critic	Linear(d_{img}, 64) + ReLU → Linear(64, 1)	$V(s_t)$=1
Initialization	Orthogonal init (all linear + embeddings)	–

Table 3: $\mathbf{RL}_{\text{f}}$ (ours) network architecture.

Component	Layer	Output dim.
Image encoder	Conv2d(3, 64, 3×3, 3) + ReLU Conv2d(64, 64, 3×3, 1) + ReLU Flatten + Linear(d_{flatten}, 64)	d_{img}=64
Text encoder	Embedding ($\|token\|$, d_{emb}=32) → Linear(32, 32)	d_{text}=32
Actor	Linear($d_{\text{img}} + d_{\text{text}}$, 64) + ReLU → Linear(64, 2)	logits (Success/Failure)=2
Critic	Linear($d_{\text{img}} + d_{\text{text}}$, 64) + ReLU → Linear(64, 1)	$V(s_{t,i})$=1
Initialization	Orthogonal init (all linear + embeddings)	–

Table 4: $\mathbf{RL}_{\text{b}}$ (baseline) network architecture.

BabyAIText. We evaluate our method on the BabyAIText environment (Paglieri et al. 2025), a two-dimensional grid world where an agent must follow natural language instructions to achieve specific goals. We focus on two task variants: *Goto* and *Pickup*. In the *Goto* task, the agent is instructed to navigate to a target object described in natural language (e.g., "go to the blue ball"). In the *Pickup* task, the agent must locate and pick up a specified object (e.g., "pick up the grey key"). Both tasks require grounding language in visual perception, spatial reasoning, and sequential planning. Each episode is generated with random object types and colors to provide a diverse and challenging set of scenarios for both training and evaluation.

Prompts for Expert Data Acquisition

NumberLine

Prompt:

```
Game: NumberLine-v0 { Visual Number
↪  Line Game (goal: reach the target
↪  position).

Observation:
- The screen displays a horizontal
↪  number line.
- The 'target position' and the
↪  'current position' are indicated
↪  by labeled text rendered along
↪  this line.
- There is no direct access to the
↪  numeric positions|you must infer
↪  the current and target locations
↪  by reading the text in the image.

Condition Under Evaluation:
↪  '<node.function>'
Your task is to determine whether this
↪  condition is TRUE or FALSE based
↪  on the current visual observation.

Previous Reasoning:
<previous_thought>

Reasoning Guidelines:
1. Read and interpret the labeled
↪  'Target' and 'Current' positions
↪  shown on the number line.
2. Determine whether the current
↪  position is to the left or right
↪  of the target.
3. Use this understanding to evaluate
↪  whether the condition logically
↪  matches what is visible.
4. Only return 'True' if the image
↪  clearly supports the condition
↪  being evaluated.

Respond ONLY in the following JSON
↪  format:
{
```

Category	Parameter	Value
General	Image Size	128
	Image Num. Channels	3
	Image Feature Dim.	64
	Text Feature Dim.	32
	Actor/Critic Dim.	64
	Frame Seq. Length	1
	Frameskip	1
Training (RL)	Epochs	4
	Batch Size	256
	Iterations	200 (NL, BJ) 500 (Others)
	Max Episode Steps	100
	Rollout Steps	$T = 2000$ (env steps; factorized RL) $K = \sum_{t=1}^{T} n_t$ (b-RL, baseline)
	Learning Rate (LR)	5×10^{-5}
	LR Scheduler	True
b-RL/RL Loss	Discount Factor γ	0.99
	GAE λ	0.95
	Value Loss Coef.	0.5
	Entropy Coef.	0.05
	Clip Epsilon	0.2
	Cross-Entropy Coef.	0.1 or 1.0
Supervised	Sup. Batch Size	64
	Sup. Epochs	100
	Sup. Patience	30
	Sup. Learning Rate	1×10^{-4}
DAgger	Iteration Budget Quota	100 (NL, FL4x4) 1,000 (Others)
	Initial Beta	1.0
	Decay α	0.95
Evaluation	Eval. Episodes	100
	Eval. Interval	10
	Eval. Greedy	True
Expert	Expert Budget (API Calls)	1,000 (NL, FL4x4) 10,000 (Others)

Table 5: Key hyperparameters used in all experiments.

```
  "thought": "<Step-by-step
  ↪  reasoning>",
  "action": "<True or False>"
}
```

Blackjack

Prompt:

```
Game: Blackjack-v0 { Visual Blackjack
↪  Game (goal: get closer to 21 than
↪  the dealer).

Observation:
- The top part of the image shows the
↪  dealer's visible card.
- The bottom part shows the player's
↪  current hand.
- There is no numerical input. You
↪  must infer hand values from card
↪  visuals.
- Face cards (J, Q, K) count as 10.
↪  Ace can count as either 1 or 11.

Condition Under Evaluation:
↪  '<node.function>'
Your task is to determine whether this
↪  condition is TRUE or FALSE in the
↪  current state.

Previous Reasoning:
<previous_thought>

Reasoning Guidelines:
1. Identify the dealer's visible card
↪  and assess its strength.
```

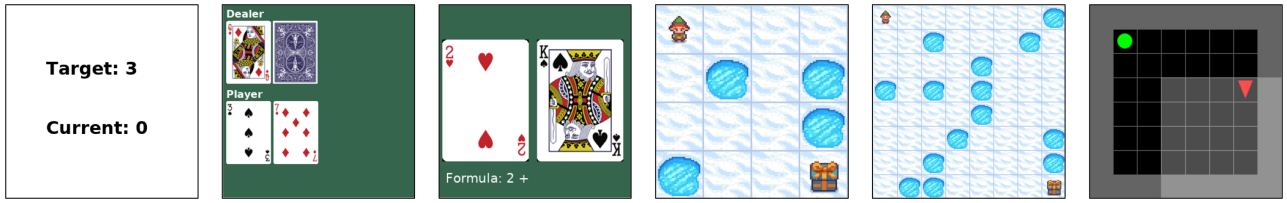

NumberLine | BlackJack | EZPoints | FrozenLake 4x4 | FrozenLake 8x8 | BabyAIText Goto/Pickup

Figure 4: Illustrations of the experimental environments. From left to right: (1) **NumberLine**, increment or decrement the counter to match a target; (2) **BlackJack**, decide to "hit" or "stand" based on visible and hidden cards; (3) **EZPoints**, build an arithmetic expression from shown cards to match a target value; (4) **FrozenLake 4x4**, navigate a small frozen grid to the goal while avoiding holes; (5) **FrozenLake 8x8**, a larger and more challenging variant; (6) **BabyAIText Goto/Pickup**, perform language-guided navigation and object manipulation in a grid world.

(a) Initial step: No tokens selected. (b) After selecting digit '2'. (c) After selecting '+'.

Figure 5: Example trajectory in *EZPoints*. The agent constructs an arithmetic formula step-by-step using visual input. It first selects a digit (b), then an operator (c), and continues until the expression reaches the target value. The final step involves selecting the equals token (=) to submit the completed formula.

```
2. Visually estimate the player's hand
↪  value using the visible cards.
3. Evaluate whether the condition
↪  description logically matches the
↪  current visual state.
4. Only return 'True' if the visual
↪  evidence clearly supports the
↪  condition.

Respond ONLY in the following JSON
↪  format:
{
  "thought": "<Step-by-step
  ↪  reasoning>",
  "action": "<True or False>"
}
```

EZPoints

Prompt:

```
Game: EZPoints-v0 { Card-Based
↪  Arithmetic Game (goal: evaluate to
↪  exactly 12).

Objective:
- Construct a valid arithmetic
↪  expression by selecting cards one
↪  at a time.
- Expressions must use visible cards
↪  (digits 1{10) and operators (+, *,
↪  =).
- Use '=' only if the formula is
↪  complete and expected to evaluate
↪  to 12.
- A maximum of 5 tokens can be
↪  selected (e.g., '4 + 8').

Game Rules:
- Number cards must match one of the
↪  visible cards and cannot repeat.
- Operators can only appear between
↪  valid numbers and must follow the
↪  formula logic.
- '=' is only valid if the formula
↪  includes at least two numbers and
↪  one operator.
- Face cards (J, Q, K) count as 10.

Rewards:
```

```
- +10 if '=' is selected and formula
↪  evaluates to exactly 12.
- {1 for invalid actions (e.g.,
↪  repeated card, premature '=')
-  0 for valid intermediate steps.

Condition Under Evaluation:
↪  '<node.function>'
Your task is to determine whether this
↪  condition is TRUE or FALSE in the
↪  current state.

Previous Reasoning:
<previous_thought>

Reasoning Guidelines:
1. Assess if the condition logically
↪  fits the current formula and
↪  visible cards.
2. Only return 'True' if the condition
↪  leads to a valid and useful next
↪  step.
3. Use visual and textual cues from
↪  the image (card layout, formula
↪  progress).

Respond ONLY in the following JSON
↪  format:
{
  "thought": "<Step-by-step
  ↪  reasoning>",
  "action": "<True or False>"
}
```

FrozenLake 4x4

Prompt:

```
Game: FrozenLake-v1 on a 4x4 grid
↪  (goal at (3,3)).
Coordinate System: (0, 0) is top-left.
↪  Format is (row, column).
Row increases ↓, Column increases →.

Grid Information:
- S = Start (safe),
- F = Frozen tile (safe),
- H = Hole (dangerous),
- G = Goal (target destination).

- (0,0)=S, (0,1)=F, (0,2)=F, (0,3)=H
- (1,0)=F, (1,1)=F, (1,2)=F, (1,3)=H
- (2,0)=F, (2,1)=H, (2,2)=F, (2,3)=H
- (3,0)=H, (3,1)=F, (3,2)=F, (3,3)=G
- Agent is currently at (row <row>,
↪  column <col>), standing on tile
↪  '<tile>'.

Objective:
- Reach the goal tile (G) at (3,3)
↪  safely and efficiently.

Previous Actions:
- <previous 4 actions>

Reasoning Guidelines:
- Only RIGHT, DOWN, LEFT, or UP moves
↪  are allowed at each step (diagonal
↪  or jumping moves are not
↪  permitted).
Question: Based on the above, is the
↪  condition '<node.function>' true?

Respond ONLY in the following JSON
↪  format:
{
  "thought": "<Step-by-step
  ↪  justification based on reasoning
  ↪  guidelines>",
  "action": "<True or False>"
}
```

FrozenLake 8x8

Prompt:

```
Game: FrozenLake-v1 on an 8×8 grid
↪  (goal at (7,7)).
Coordinate System: (0, 0) is top-left.
↪  Format is (row, column).
Row increases ↓, Column increases →.

Grid Information:
- S = Start (safe),
- F = Frozen tile (safe),
- H = Hole (dangerous),
- G = Goal (target destination).

- (0,0)=S, (0,1)=F, (0,2)=F, (0,3)=F,
↪  (0,4)=F, (0,5)=F, (0,6)=F, (0,7)=H
- (1,0)=F, (1,1)=F, (1,2)=H, (1,3)=F,
↪  (1,4)=F, (1,5)=H, (1,6)=F, (1,7)=H
- (2,0)=F, (2,1)=F, (2,2)=F, (2,3)=F,
↪  (2,4)=H, (2,5)=F, (2,6)=F, (2,7)=F
- (3,0)=H, (3,1)=H, (3,2)=F, (3,3)=H,
↪  (3,4)=F, (3,5)=F, (3,6)=F, (3,7)=H
- (4,0)=F, (4,1)=F, (4,2)=F, (4,3)=F,
↪  (4,4)=F, (4,5)=H, (4,6)=F, (4,7)=F
- (5,0)=F, (5,1)=H, (5,2)=F, (5,3)=F,
↪  (5,4)=F, (5,5)=F, (5,6)=H, (5,7)=F
- (6,0)=F, (6,1)=F, (6,2)=F, (6,3)=F,
↪  (6,4)=H, (6,5)=F, (6,6)=F, (6,7)=H
- (7,0)=F, (7,1)=H, (7,2)=F, (7,3)=H,
↪  (7,4)=F, (7,5)=F, (7,6)=F, (7,7)=G
- Agent is currently at (row <row>,
↪  column <col>), standing on tile
↪  '<tile>'.

Objective:
- Reach the goal tile (G) at (7,7)
↪  safely and efficiently.

Previous Actions:
- <previous 4 actions>
```

```
Reasoning Guidelines:
- Only RIGHT, DOWN, LEFT, or UP moves
 ↪  are allowed at each step (diagonal
 ↪  or jumping moves are not
 ↪  permitted).
Question: Based on the above, is the
 ↪  condition '<node.function>' true?

Respond ONLY in the following JSON
 ↪  format:
{
  "thought": "<Step-by-step
   ↪  justification based on reasoning
   ↪  guidelines>",
  "action": "<True or False>"
}
```

BabyAIText Goto

Prompt:

```
Game: BabyAIText-v0 { Grid World with
 ↪  Language Instructions.

Mission: <mission text>
Coordinate System: (0, 0) is top-left.
 ↪  Format is (row, column).
Row increases ↓, Column increases →.
Agent Position: <row, col>, Facing:
 ↪  <direction>
Visible Objects:
- <object list, e.g., "green box at
 ↪  (1,2)" ...>

Scene Description: <long term context
 ↪  from environment>
Possible Actions: <action_1>,
 ↪  <action_2>, ...

Condition Under Evaluation:
 ↪  '<node.function>'
Your task is to determine whether this
 ↪  condition is TRUE or FALSE in the
 ↪  current state.

Reasoning Guidelines:
0. The agent is shaped like a
 ↪  triangle. The pointed tip of the
 ↪  triangle indicates the direction
 ↪  it is facing (e.g., North, South,
 ↪  East, West). 'Turn left' means
 ↪  rotating the triangle (agent) 90
 ↪  degrees counterclockwise, and
 ↪  'Turn right' means rotating it 90
 ↪  degrees clockwise, relative to the
 ↪  direction the tip is pointing.
1. Directional terms like 'Left' and
 ↪  'Right' are defined strictly
 ↪  relative to the agent's current
 ↪  facing direction. This means:
    - If facing North, 'left' is West
     ↪  and 'right' is East.
    - If facing East, 'left' is North
     ↪  and 'right' is South.
    - If facing South, 'left' is East
     ↪  and 'right' is West.
    - If facing West, 'left' is South
     ↪  and 'right' is North.
    * Do not confuse these with object
     ↪  positions on the map or
     ↪  coordinates like (x, y). Always
     ↪  interpret directions from the
     ↪  agent's perspective.
    For example, if the agent is facing
     ↪  South and an object is at (x+1,
     ↪  y), that object is to the
     ↪  agent's left.
2. Explore the area if there are no
 ↪  target objects mentioned in the
 ↪  Scene Description.

Respond ONLY in the following JSON
 ↪  format:
{
  "thought": "<Step-by-step
   ↪  reasoning>",
  "action": "<True or False>"
}
```

BabyAIText Pickup

Prompt:

```
Game: BabyAIText-v0 { Grid World with
 ↪  Language Instructions.

Mission: <mission text>
Coordinate System: (0, 0) is top-left.
 ↪  Format is (row, column).
Row increases ↓, Column increases →.
Agent Position: <row, col>, Facing:
 ↪  <direction>
Visible Objects:
- <object list, e.g., "green box at
 ↪  (1,2)" ...>

Scene Description: <long term context
 ↪  from environment>
Possible Actions: <action_1>,
 ↪  <action_2>, ...

Condition Under Evaluation:
 ↪  '<node.function>'
Your task is to determine whether this
 ↪  condition is TRUE or FALSE in the
 ↪  current state.

Reasoning Guidelines:
```

```
0. The agent is shaped like a
↪  triangle. The pointed tip of the
↪  triangle indicates the direction
↪  it is facing (e.g., North, South,
↪  East, West). 'Turn left' means
↪  rotating the triangle (agent) 90
↪  degrees counterclockwise, and
↪  'Turn right' means rotating it 90
↪  degrees clockwise, relative to the
↪  direction the tip is pointing.
1. An object can only be picked up if
↪  it is in the cell directly in
↪  front of the agent.
2. Some objects, such as doors, cannot
↪  be picked up. Only items like
↪  keys, boxes, or balls are
↪  pickable.
3. Directional terms like 'Left' and
↪  'Right' are defined strictly
↪  relative to the agent's current
↪  facing direction. This means:
   - If facing North, 'left' is West
   ↪  and 'right' is East.
   - If facing East, 'left' is North
   ↪  and 'right' is South.
   - If facing South, 'left' is East
   ↪  and 'right' is West.
   - If facing West, 'left' is South
   ↪  and 'right' is North.
   * Do not confuse these with object
   ↪  positions on the map or
   ↪  coordinates like (x, y). Always
   ↪  interpret directions from the
   ↪  agent's perspective.
4. Explore the area if there are no
↪  target objects mentioned in the
↪  Scene Description.

Respond ONLY in the following JSON
↪  format:
{
  "thought": "<Step-by-step
  ↪  reasoning>",
  "action": "<True or False>"
}
```

Bahavior Trees for Each Task

NumberLine

Behavior Tree:

```
{
    "type": "selector",
    "name": "Root",
    "children": [
        {
            "type": "sequence",
            "name": "Move Right
            ↪  Sequence",
            "children": [
                {
                    "type":
                    ↪  "condition",
                    "name": "Check
                    ↪  Current Less
                    ↪  Than Target",
                    "function": "Is
                    ↪  current
                    ↪  position less
                    ↪  than target?"
                },
                {
                    "type": "action",
                    "name": "Execute
                    ↪  Move Right",
                    "function":
                    ↪  "MOVE_RIGHT"
                }
            ]
        },
        {
            "type": "sequence",
            "name": "Move Left
            ↪  Sequence",
            "children": [
                {
                    "type":
                    ↪  "condition",
                    "name": "Check
                    ↪  Current
                    ↪  Greater Than
                    ↪  Target",
                    "function": "Is
                    ↪  current
                    ↪  position
                    ↪  greater than
                    ↪  target?"
                },
                {
                    "type": "action",
                    "name": "Execute
                    ↪  Move Left",
                    "function":
                    ↪  "MOVE_LEFT"
                }
            ]
        },
        {
            "type": "action",
            "name": "Default Move
            ↪  Right",
            "function": "MOVE_RIGHT"
        }
    ]
}
```

Blackjack

Behavior Tree:

```
{
  "type": "selector",
  "name": "Root",
```

```
  "children": [
    {
      "type": "sequence",
      "name": "Stick If Hand Is
      ↪  Exactly 21",
      "children": [
        {
          "type": "condition",
          "name": "Hand Equals 21",
          "function": "Is the player's
          ↪  hand exactly 21?"
        },
        {
          "type": "action",
          "name": "Select Stick",
          "function": "STICK"
        }
      ]
    },
    {
      "type": "sequence",
      "name": "Stick If Hand Is Very
      ↪  High",
      "children": [
        {
          "type": "condition",
          "name": "Hand Is 19 or 20",
          "function": "Is the player's
          ↪  hand value very high (19
          ↪  or 20)?"
        },
        {
          "type": "action",
          "name": "Select Stick",
          "function": "STICK"
        }
      ]
    },
    {
      "type": "sequence",
      "name": "Hit If Dealer Strong
      ↪  And Hand Moderate",
      "children": [
        {
          "type": "condition",
          "name": "Dealer Has Strong
          ↪  Card",
          "function": "Is the dealer's
          ↪  visible card strong (7
          ↪  to Ace)?"
        },
        {
          "type": "condition",
          "name": "Hand Is 17 or 18",
          "function": "Is the player's
          ↪  hand in moderate range
          ↪  (17 or 18)?"
        },
        {
          "type": "action",
          "name": "Select Hit",
          "function": "HIT"
        }
      ]
    },
    {
      "type": "sequence",
      "name": "Hit If Hand Low",
      "children": [
        {
          "type": "condition",
          "name": "Hand Below 17",
          "function": "Is the player's
          ↪  hand below 17?"
        },
        {
          "type": "action",
          "name": "Select Hit",
          "function": "HIT"
        }
      ]
    },
    {
      "type": "action",
      "name": "Fallback Stick",
      "function": "STICK"
    }
  ]
}
```

EZPoints

Behavior Tree:

```
{
"type": "selector",
"name": "Root",
"children": [
    {
    "type": "sequence",
    "name": "Try Finish Formula
    ↪  Correctly",
    "children": [
        {
        "type": "condition",
        "name": "Formula Ready Equals
        ↪  12",
        "function": "Is the formula
        ↪  complete and does it
        ↪  evaluate to 12?"
        },
        {
        "type": "action",
        "name": "Select Equals",
        "function": "="
        }
    ]
    },
    {
    "type": "sequence",
    "name": "Add Operator If Needed",
    "children": [
        {
        "type": "condition",
        "name": "Needs Operator",
```

```
        "function": "Does the formula
        ↪  end with a number and not
        ↪  yet have an operator?"
        },
        {
        "type": "selector",
        "name": "Choose Operator",
        "children": [
            {
            "type": "sequence",
            "name": "Try Plus",
            "children": [
                {
                "type": "condition",
                "name": "Should Use
                ↪  Plus",
                "function": "Is '+' a
                ↪  better choice
                ↪  based on remaining
                ↪  values?"
                },
                {
                "type": "action",
                "name": "Select Plus",
                "function": "+"
                }
            ]
            },
            {
            "type": "action",
            "name": "Select Multiply",
            "function": "*"
            }
        ]
        }
    ]
    },
    {
    "type": "sequence",
    "name": "Add Number If Needed",
    "children": [
        {
        "type": "condition",
        "name": "Needs Number",
        "function": "Is the formula
        ↪  empty or ends with an
        ↪  operator?"
        },
        {
        "type": "selector",
        "name": "Choose Number From
        ↪  Visible Cards",
        "children": [
            {
            "type": "sequence",
            "name": "Use 1",
            "children": [
                {
                "type": "condition",
                "name": "Can Use 1",
                "function": "Is '1'
                ↪  visible in cards
                ↪  and not in the
                ↪  formula?"
                },
                {
                "type": "action",
                "name": "Select 1",
                "function": "1"
                }
            ]
            },
            {
            "type": "sequence",
            "name": "Use 2",
            "children": [
                {
                "type": "condition",
                "name": "Can Use 2",
                "function": "Is '2'
                ↪  visible in cards
                ↪  and not in the
                ↪  formula?"
                },
                {
                "type": "action",
                "name": "Select 2",
                "function": "2"
                }
            ]
            },
            {
            "type": "sequence",
            "name": "Use 3",
            "children": [
                {
                "type": "condition",
                "name": "Can Use 3",
                "function": "Is '3'
                ↪  visible in cards
                ↪  and not in the
                ↪  formula?"
                },
                {
                "type": "action",
                "name": "Select 3",
                "function": "3"
                }
            ]
            },
            {
            "type": "sequence",
            "name": "Use 4",
            "children": [
                {
                "type": "condition",
                "name": "Can Use 4",
                "function": "Is '4'
                ↪  visible in cards
                ↪  and not in the
                ↪  formula?"
                },
                {
```

```
            "type": "action",
            "name": "Select 4",
            "function": "4"
            }
        ]
        },
        {
        "type": "sequence",
        "name": "Use 5",
        "children": [
            {
            "type": "condition",
            "name": "Can Use 5",
            "function": "Is '5'
            ↪  visible in cards
            ↪  and not in the
            ↪  formula?"
            },
            {
            "type": "action",
            "name": "Select 5",
            "function": "5"
            }
        ]
        },
        {
        "type": "sequence",
        "name": "Use 6",
        "children": [
            {
            "type": "condition",
            "name": "Can Use 6",
            "function": "Is '6'
            ↪  visible in cards
            ↪  and not in the
            ↪  formula?"
            },
            {
            "type": "action",
            "name": "Select 6",
            "function": "6"
            }
        ]
        },
        {
        "type": "sequence",
        "name": "Use 7",
        "children": [
            {
            "type": "condition",
            "name": "Can Use 7",
            "function": "Is '7'
            ↪  visible in cards
            ↪  and not in the
            ↪  formula?"
            },
            {
            "type": "action",
            "name": "Select 7",
            "function": "7"
            }
        ]
        },
```

```
            {
            "type": "sequence",
            "name": "Use 8",
            "children": [
                {
                "type": "condition",
                "name": "Can Use 8",
                "function": "Is '8'
                ↪  visible in cards
                ↪  and not in the
                ↪  formula?"
                },
                {
                "type": "action",
                "name": "Select 8",
                "function": "8"
                }
            ]
            },
            {
            "type": "sequence",
            "name": "Use 9",
            "children": [
                {
                "type": "condition",
                "name": "Can Use 9",
                "function": "Is '9'
                ↪  visible in cards
                ↪  and not in the
                ↪  formula?"
                },
                {
                "type": "action",
                "name": "Select 9",
                "function": "9"
                }
            ]
            },
            {
            "type": "sequence",
            "name": "Use 10",
            "children": [
                {
                "type": "condition",
                "name": "Can Use 10",
                "function": "Is '10'
                ↪  visible in cards
                ↪  and not in the
                ↪  formula?"
                },
                {
                "type": "action",
                "name": "Select 10",
                "function": "10"
                }
            ]
            }
        ]
        }
    ]
    },
    {
    "type": "sequence",
```

```
    "name": "Force Finish If Out Of
    ↪  Tokens",
    "children": [
        {
        "type": "condition",
        "name": "Formula At Max
        ↪  Tokens",
        "function": "Is the formula at
        ↪  5 tokens and not yet
        ↪  evaluated?"
        },
        {
        "type": "action",
        "name": "Force Equals",
        "function": "="
        }
    ]
    },
    {
    "type": "action",
    "name": "Default Select Equals",
    "function": "="
    }
]
}
```

FrozenLake 4x4 / 8x8

Behavior Tree:

```
{
  "type": "selector",
  "name": "Root",
  "children": [
    {
      "type": "sequence",
      "name": "Move RIGHT if Safe and
      ↪  Valid Path",
      "children": [
        {
          "type": "condition",
          "name": "RIGHT is non-hole",
          "function": "Does moving
          ↪  RIGHT lead to a non-hole
          ↪  tile?"
        },
        {
          "type": "condition",
          "name": "RIGHT is on valid
          ↪  path",
          "function": "Is the next
          ↪  tile after moving RIGHT
          ↪  not surrounded on three
          ↪  sides by holes or by
          ↪  holes and walls, can you
          ↪  immediately continue
          ↪  moving down or right
          ↪  from there to reach the
          ↪  goal, and does this move
          ↪  avoid repeatedly
          ↪  alternating between two
          ↪  actions (such as [RIGHT,
          ↪  LEFT] followed by
          ↪  another RIGHT)?"
        },
        {
          "type": "action",
          "name": "Move RIGHT",
          "function": "RIGHT"
        }
      ]
    },
    {
      "type": "sequence",
      "name": "Move DOWN if Safe and
      ↪  Valid Path",
      "children": [
        {
          "type": "condition",
          "name": "DOWN is non-hole",
          "function": "Does moving
          ↪  DOWN lead to a non-hole
          ↪  tile?"
        },
        {
          "type": "condition",
          "name": "DOWN is on valid
          ↪  path",
          "function": "Is the next
          ↪  tile after moving DOWN
          ↪  not surrounded on three
          ↪  sides by holes or by
          ↪  holes and walls, can you
          ↪  immediately continue
          ↪  moving down or right
          ↪  from there to reach the
          ↪  goal, and does this move
          ↪  avoid repeatedly
          ↪  alternating between two
          ↪  actions (such as [DOWN,
          ↪  UP] followed by another
          ↪  DOWN)?"
        },
        {
          "type": "action",
          "name": "Move DOWN",
          "function": "DOWN"
        }
      ]
    },
    {
      "type": "sequence",
```

```
      "name": "Move LEFT if Safe and
      ↪  Valid Path",
      "children": [
        {
          "type": "condition",
          "name": "LEFT is non-hole",
          "function": "Does moving
          ↪  LEFT lead to a non-hole
          ↪  tile?"
        },
        {
          "type": "condition",
          "name": "LEFT is on valid
          ↪  path",
          "function": "Is the next
          ↪  tile after moving LEFT
          ↪  not surrounded on three
          ↪  sides by holes or by
          ↪  holes and walls, can you
          ↪  immediately continue
          ↪  moving down or right
          ↪  from there to reach the
          ↪  goal, and does this move
          ↪  avoid repeatedly
          ↪  alternating between two
          ↪  actions (such as [LEFT,
          ↪  RIGHT] followed by
          ↪  another LEFT)?"
        },
        {
          "type": "action",
          "name": "Move LEFT",
          "function": "LEFT"
        }
      ]
    },
    {
      "type": "sequence",
      "name": "Move UP if Safe and
      ↪  Valid Path",
      "children": [
        {
          "type": "condition",
          "name": "UP is non-hole",
          "function": "Does moving UP
          ↪  lead to a non-hole
          ↪  tile?"
        },
        {
          "type": "condition",
          "name": "UP is on valid
          ↪  path",
          "function": "Is the next
          ↪  tile after moving UP not
          ↪  surrounded on three
          ↪  sides by holes or by
          ↪  holes and walls, can you
          ↪  immediately continue
          ↪  moving down or right
          ↪  from there to reach the
          ↪  goal, and does this move
          ↪  avoid repeatedly
          ↪  alternating between two
          ↪  actions (such as [UP,
          ↪  DOWN] followed by
          ↪  another UP)?"
        },
        {
          "type": "action",
          "name": "Move UP",
          "function": "UP"
        }
      ]
    },
    {
      "type": "action",
      "name": "Default Action (LEFT)",
      "function": "LEFT"
    }
  ]
}
```

BabyAIText Goto

Behavior Tree:

```
{
  "type": "selector",
  "name": "Root",
  "children": [
    {
      "type": "sequence",
      "name": "Move Forward Toward
      ↪  Target",
      "children": [
        {
          "type": "condition",
          "name": "Target Ahead",
          "function": "Is the target
          ↪  object located somewhere
          ↪  in front of the agent
          ↪  (not 0 steps forward),
          ↪  possibly with a few
          ↪  steps left or right
          ↪  relative to its facing
          ↪  direction? (e.g., x
          ↪  steps left/right and y
          ↪  steps forward)?"
        },
        {
          "type": "condition",
          "name": "Immediate Step
          ↪  Clear",
```

```
        "function": "Is the cell one
        ↪  step ahead of the agent
        ↪  clear (i.e., no object
        ↪  listed at that position
        ↪  in 'Visible Objects')?"
      },
      {
        "type": "action",
        "name": "Move Forward",
        "function": "go forward"
      }
    ]
  },

  {
    "type": "sequence",
    "name": "Rotate Left Toward
    ↪  Target",
    "children": [
      {
        "type": "condition",
        "name": "Need To Turn Left",
        "function": "Is the target
        ↪  object located to the
        ↪  agent's left side (0~90
        ↪  degrees
        ↪  counterclockwise) from
        ↪  its current facing
        ↪  direction?"
      },
      {
        "type": "action",
        "name": "Turn Left",
        "function": "turn left"
      }
    ]
  },

  {
    "type": "sequence",
    "name": "Rotate Right Toward
    ↪  Target",
    "children": [
      {
        "type": "condition",
        "name": "Need To Turn
        ↪  Right",
        "function": "Is the target
        ↪  object located to the
        ↪  agent's right side (0~90
        ↪  degrees clockwise) from
        ↪  its current facing
        ↪  direction?"
      },
      {
        "type": "action",
        "name": "Turn Right",
        "function": "turn right"
      }
    ]
  },

  {
```

```
    "type": "selector",
    "name": "Exploration (Optimal
    ↪  Default Action)",
    "children": [
      {
        "type": "sequence",
        "name": "Explore Left
        ↪  Required",
        "children": [
          {
            "type": "condition",
            "name": "Turn Left
            ↪  Toward Target?",
            "function": "Is turning
            ↪  left (90 degrees
            ↪  counterclockwise,
            ↪  possibly multiple
            ↪  times) required
            ↪  among the possible
            ↪  actions to reach the
            ↪  target object?"
          },
          {
            "type": "action",
            "name": "Turn Left",
            "function": "turn left"
          }
        ]
      },
      {
        "type": "sequence",
        "name": "Explore Right
        ↪  Required",
        "children": [
          {
            "type": "condition",
            "name": "Turn Right
            ↪  Toward Target?",
            "function": "Is turning
            ↪  right (90 degrees
            ↪  clockwise, possibly
            ↪  multiple times)
            ↪  required among the
            ↪  possible actions to
            ↪  reach the target
            ↪  object?"
          },
          {
            "type": "action",
            "name": "Turn Right",
            "function": "turn right"
          }
        ]
      },
      {
        "type": "sequence",
        "name": "Explore Forward
        ↪  Required",
        "children": [
          {
            "type": "condition",
            "name": "Go Forward
            ↪  Toward Target?",
```

```
              "function": "Is going
              ↪  forward required
              ↪  among the possible
              ↪  actions to reach the
              ↪  target object?"
            },
            {
              "type": "action",
              "name": "Go Forward",
              "function": "go forward"
            }
          ]
        }
      ]
    },
    {
      "type": "action",
      "name": "Default Action (Turn
      ↪  Left)",
      "function": "turn left"
    }
  ]
}
```

BabyAIText Pickup

Behavior Tree:

```
{
  "type": "selector",
  "name": "Root",
  "children": [
    {
      "type": "sequence",
      "name": "Pick Up Target If In
      ↪  Front",
      "children": [
        {
          "type": "condition",
          "name": "Target Directly
          ↪  Ahead",
          "function": "Is the target
          ↪  object located in the
          ↪  cell directly in front
          ↪  of the agent?"
        },
        {
          "type": "action",
          "name": "Pick Up",
          "function": "pick up"
        }
      ]
    },

    {
      "type": "sequence",
      "name": "Move Forward Toward
      ↪  Target",
      "children": [
        {
          "type": "condition",
          "name": "Target Ahead",
          "function": "Is the target
          ↪  object located somewhere
          ↪  in front of the agent
          ↪  (not 0 steps forward),
          ↪  possibly with a few
          ↪  steps left or right
          ↪  relative to its facing
          ↪  direction? (e.g., x
          ↪  steps left/right and y
          ↪  steps forward)?"
        },
        {
          "type": "condition",
          "name": "Immediate Step
          ↪  Clear",
          "function": "Is the cell one
          ↪  step ahead of the agent
          ↪  clear (i.e., no object
          ↪  listed at that position
          ↪  in 'Visible Objects')?"
        },
        {
          "type": "action",
          "name": "Move Forward",
          "function": "go forward"
        }
      ]
    },

    {
      "type": "sequence",
      "name": "Rotate Left Toward
      ↪  Target",
      "children": [
        {
          "type": "condition",
          "name": "Need To Turn Left",
          "function": "Is the target
          ↪  object located to the
          ↪  agent's left side (0˜90
          ↪  degrees
          ↪  counterclockwise) from
          ↪  its current facing
          ↪  direction?"
        },
        {
          "type": "action",
          "name": "Turn Left",
          "function": "turn left"
        }
      ]
    },

    {
      "type": "sequence",
      "name": "Rotate Right Toward
      ↪  Target",
      "children": [
        {
          "type": "condition",
          "name": "Need To Turn
          ↪  Right",
```

```
          "function": "Is the target
          ↪  object located to the
          ↪  agent's right side (0~90
          ↪  degrees clockwise) from
          ↪  its current facing
          ↪  direction?"
        },
        {
          "type": "action",
          "name": "Turn Right",
          "function": "turn right"
        }
      ]
    },

    {
      "type": "selector",
      "name": "Exploration (Optimal
      ↪  Default Action)",
      "children": [
        {
          "type": "sequence",
          "name": "Explore Left
          ↪  Required",
          "children": [
            {
              "type": "condition",
              "name": "Turn Left
              ↪  Toward Target?",
              "function": "Is turning
              ↪  left (90 degrees
              ↪  counterclockwise,
              ↪  possibly multiple
              ↪  times) required
              ↪  among the possible
              ↪  actions to reach the
              ↪  target object?"
            },
            {
              "type": "action",
              "name": "Turn Left",
              "function": "turn left"
            }
          ]
        },
        {
          "type": "sequence",
          "name": "Explore Right
          ↪  Required",
          "children": [
            {
              "type": "condition",
              "name": "Turn Right
              ↪  Toward Target?",
              "function": "Is turning
              ↪  right (90 degrees
              ↪  clockwise, possibly
              ↪  multiple times)
              ↪  required among the
              ↪  possible actions to
              ↪  reach the target
              ↪  object?"
            },
            {
              "type": "action",
              "name": "Turn Right",
              "function": "turn right"
            }
          ]
        },
        {
          "type": "sequence",
          "name": "Explore Forward
          ↪  Required",
          "children": [
            {
              "type": "condition",
              "name": "Go Forward
              ↪  Toward Target?",
              "function": "Is going
              ↪  forward required
              ↪  among the possible
              ↪  actions to reach the
              ↪  target object?"
            },
            {
              "type": "action",
              "name": "Go Forward",
              "function": "go forward"
            }
          ]
        }
      ]
    },
    {
      "type": "action",
      "name": "Default Action (Turn
      ↪  Left)",
      "function": "turn left"
    }
  ]
}
```

Visualization of Behavior Trees for each task

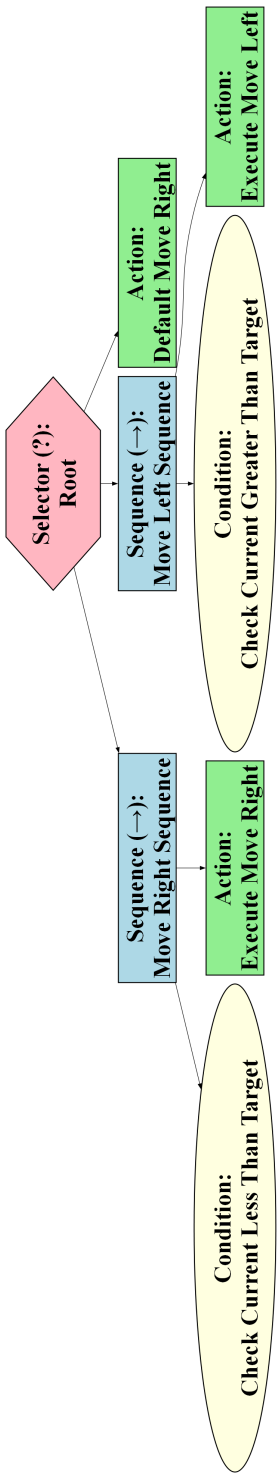

Figure 6: NumberLine

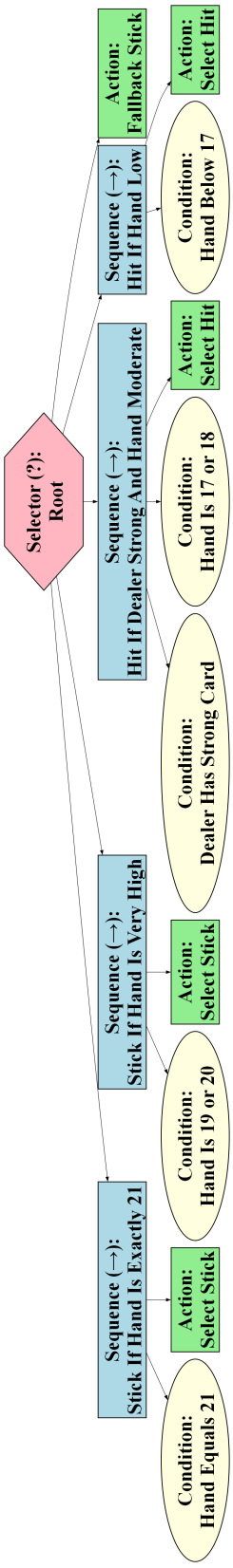

Figure 7: BlackJack

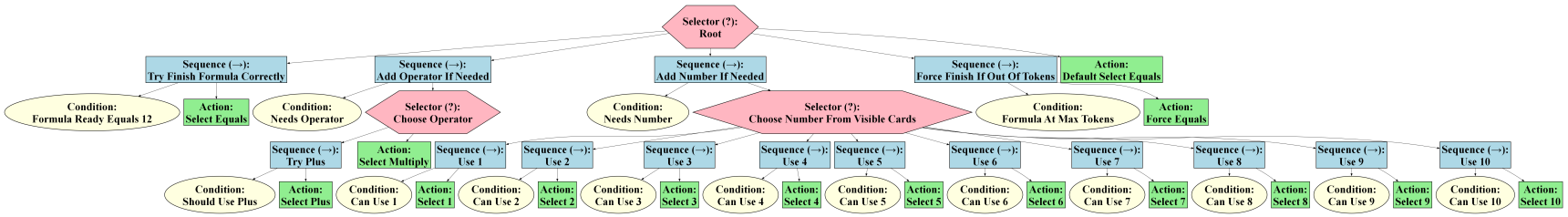

Figure 8: EZPoints

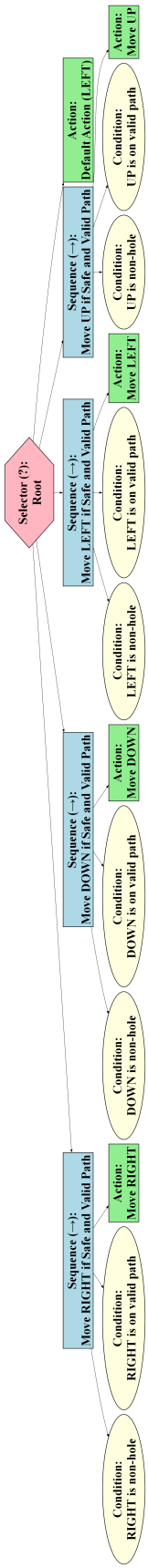

Figure 9: FrozenLake 4x4 / 8x8

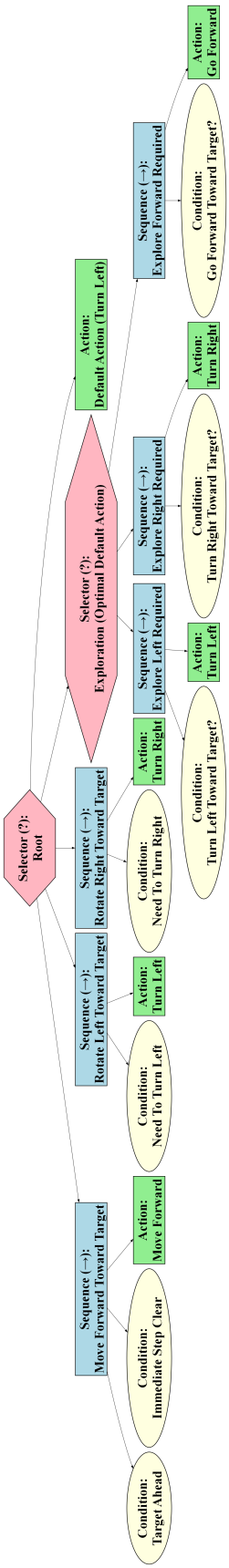

Figure 10: BabyAIText Goto

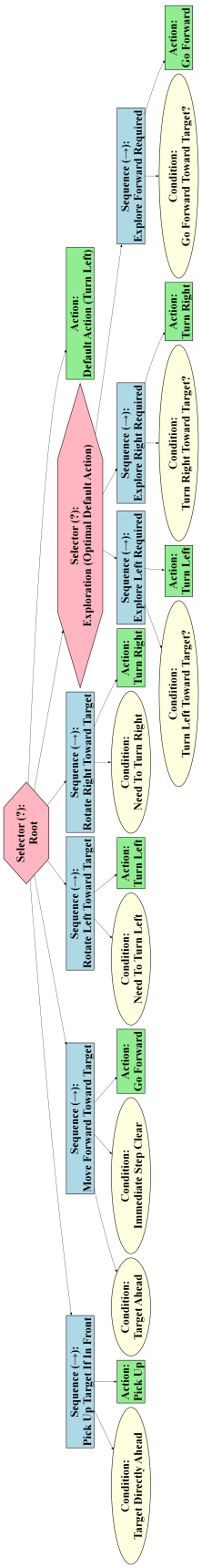

Figure 11: BabyAIText Pickup